Alma Mater Studiorum · Università di Bologna

Scuola di Scienze
Dipartimento di Fisica e Astronomia
Corso di Laurea Magistrale in Fisica

Persistent currents in a Fermi gas confined on a ring shaped potential

Relatore:
Prof.ssa Elisa Ercolessi

Correlatore:
Dott.ssa Anna Minguzzi
Dott. Piero Naldesi

Presentata da:
Giovanni Pecci

Anno Accademico 2018/2019

Abstract

This thesis aims to study an ultracold atoms Fermi gas confined on a ring-shaped potential and subjected to attractive contact interactions. In particular, we focus on the analysis of the continuous crossover between the weakly interacting regime, in which the ground state of the system is composed of weakly bound paired fermions and the strongly interacting regime, in which the tight bounds among the atoms allow to neglect the fermionic nature of the pairs. In this limit, the particles can be effectively considered as point-like bosons. In order to determine some observables that keep track of the different regimes of this crossover, we consider an artificial gauge field acting on the gas: the latter induces a persistent current in the ring that presents a periodic behaviour with respect to the artificial gauge flux. The exact solution to this model is provided using Bethe Ansatz and the periodicity can be determined at any interaction strength. Afterwards, we study in detail the number parity effect, that is measurable at low interactions and vanishes in the high interacting bosonic limit of the model, as we expect from the general theory. Such parity effect, that can be detected studying the behaviour of the persistent current, results to be a useful tool to probe the different regimes of the crossover, providing a well-defined distinction between the fermionic and the bosonic limit of the gas.

Sommario

Lo scopo di tale trattazione è lo studio di un gas di Fermi di atomi ultrafreddi confinato su un anello ed in presenza di interazioni di contatto attrattive. In particolare ci si è concentrati sullo studio dettagliato del crossover fra il regime debolmente interagente, in cui il ground state del sistema è formato da coppie di atomi debolmente legate e il regime fortemente interagente, in cui l'energia di legame di tali coppie risulta essere talmente alta che la loro natura fermionica può essere completamente trascurata. In questo limite le particelle del gas possono essere effettivamente trattate come bosoni puntiformi. Al fine di determinare degli osservabili in grado di definire con esattezza i diversi regimi di tale crossover, si è considerata l'azione di un campo di gauge artificiale agente sul gas, il quale induce una corrente di massa non dissipativa nell'anello. Tale corrente, non nulla solo su scala mesoscopica, presenta una periodicità nei confronti del flusso artificiale di campo di gauge. La soluzione esatta a tale sistema può essere determinata tramite Bethe Ansatz e la periodicità viene ricavata per ogni valore della costante di accoppiamento. In seguito viene studiato nel dettaglio l'effetto di parità dipendente dal numero di particelle del sistema, il quale risulta osservabile a basse interazioni e svanisce nel limite bosonico altamente interagente descritto sopra, in accordo con la teoria e la letteratura generale presente sull'argomento. Tale effetto di parità, che può essere rilevato a partire dalla citata periodicità della corrente persistente, risulta dunque essere un buon indicatore dei diversi regimi del crossover, permettendo di distinguere fra limite fermionico e bosonico del gas.

Contents

Introduction

Since the second half of the previous century, in particular after the realization of the first Bose-Einstein condensate in 1995 by Cornell and Wieman[1], ultracold gases have played a very rich and important role in modern physical research, both from a theoretical and experimental point of view. The physical realization of such systems, together with the evolution in optical and magnetic trapping techniques implemented to confine atomic gases in one-dimensional geometries, have encouraged an increasing and dense theoretical activity in this field. Indeed low dimensionality provides fascinating scenarios in which the interaction among the components of the system produces extremely non-trivial effects, to be combined with a mathematical formalism that is far more accessible if compared with the higher dimensional models.

One of the most ambitious applications of the physics of ultracold atoms is Atomtronics[2]. This emerging field of research aims to provide an atomic analog to electronic circuits and devices. The advantages of this alternative approach, that targets both classical and quantum-based electronics, rely on a more various nature of the particles used for circuitry. Indeed, using ultracold atoms allows to deal with both bosonic and fermionic carriers that can be coupled via a wide variety of interactions that can be tuned with great accuracy.

There are several ways to simulate a system of charged particles using atoms [3]: one of the most common is to trap the latters in a ring-shaped potential and then make the system to rotate. Indeed, as will be shown in Chapter 3, exploiting the similarity between the Hamiltonian terms describing respectively the Lorentz and the Coriolis forces, one can formally reproduce the behaviour of charged particles in a magnetic field studying the rotating system of ultracold atoms. This tool introduces a non-dissipative mass current in the ring that can be used to probe some of the microscopic properties of the system. It's worthy to notice that such current is a purely mesoscopic effect and it's not observable in the thermodynamic limit. As a consequence, the finite size of the ring represents an important feature for this kind of analysis.

The applications of Atomtronics range from the simulations of quantum systems [4], exploiting the ring geometry to reduce the problems related to the boundary effects, to the realization of integrated circuits [5] and high-precision sensing devices such as quantum interferometers [6]. At the moment, the great part of the research and experiments

in Atomtronics concern bosonic systems. Among the main purposes of this thesis, there is the attempt to introduce fermionic atoms in this framework and to study some typical phenomena of these systems using artificial gauge fields and the consequent persistent current at the equilibrium. The reasons for opening this new branch are also related to an increasing experimental interest in Fermi Atomtronics systems.

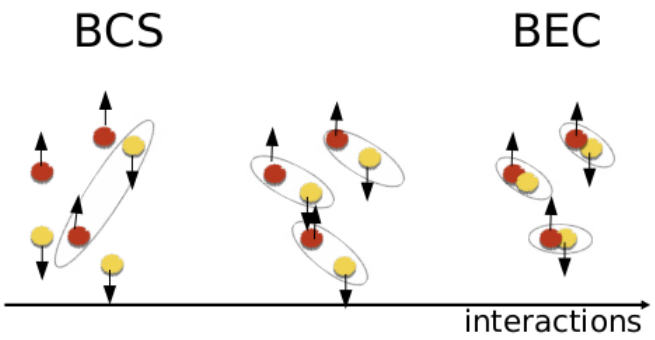

Figure 1: Qualitative picture of BCS-BEC crossover: at low attractive interactions the Fermi gas is composed by weak bound paired atoms. Increasing the interaction strength one reduces the dimension of the pairs towards a regime in which strong attractions allow to consider them as point-like bosons.

An interesting phenomenon that occurs in fermionic systems is the so-called BCS-BEC crossover[7], qualitatively pictured in Fig.1. Consider a Fermi gas subjected to an attractive contact interaction in three dimensions: the configuration of the ground state depends on the coupling strength. Indeed, at low interactions, the gas is composed of weakly bound Cooper-like pairs, whose size is larger than the interparticle spacing. This makes the pairs to overlap in this regime, called the BCS side of the crossover. Increasing the interaction strength, the system is driven through a regime of tightly bound fermions in which there's no spatial overlapping between the pairs. In this regime, called BEC side, the strong attractions between the atoms allow the formation of dimers whose internal fermionic structure can be neglected and the particles behave as point-like bosons.

In three dimensions the residual coupling between the dimers results in a finite repulsion due to the Pauli principle and below a critical temperature the system achieves Bose-Einstein condensation[8]. As we will see, this property depends on the confinement applied to the gas: the interactions in the bosonic limit of the model are different in lower dimensions and the condensation doesn't always occur.

The experimental technique used to drive the system through the different regimes of the crossover is the Feshbach resonance, that allows to change the interaction between two species of fermionic atoms by applying an external magnetic field. Indeed, the latter provides the ability to continuously tune the scattering length of a two-particle scattering process that univocally defines the scattering amplitude at low energy scales. More details about Feshbach resonance can be found in reference [9].

The three-dimensional theoretical model that describes the BCS-BEC crossover is not exactly solvable: one of the purposes of this thesis is to find a one dimensional and integrable fermionic model that describes such phenomenon following some indications already present in literature[10]. Afterwards, we want to characterize the different regimes

probing the response of the system to an external artificial gauge field determining some observables that keep track of the fermionic or bosonic nature of the components of the gas with respect to interactions.

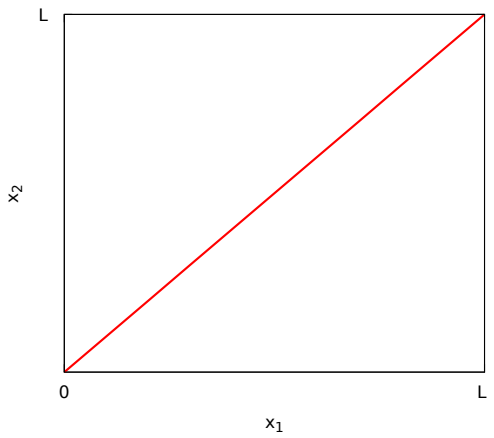

Figure 2: Domain of the spatial eigenfunction of a one-dimensional system subject to a delta interaction for $N = 2$ particles. We can see that it can be divided in two subdomains in which the particles are non-interacting: the delta potential is non-vanishing only on the edge $x_1 = x_2$ indicated by the red line and can be implemented imposing suitable boundary conditions.

One of the most efficient theoretical approaches for the exact solution of models describing one-dimensional quantum gases is the Bethe Ansatz[11]. This technique provides an explicit and very general expression for the solution of the Schroedinger equation related to an N-body Hamiltonian in which interactions can be implemented by imposing additional conditions on the formal structure of the non-interacting eigenfunction. This procedure reduces the complexity of the problem, allowing the system to be studied in a free regime with some auxiliary constraints that typically assume the form of polynomial or transcendental equations.
An example of coupling that can be treated via Bethe Ansatz is the contact interaction, that can be described by a delta function of the distances between the particles. Indeed, from the general quantum theory of one-dimensional systems, it is well known that such interaction can be equivalently implemented by requiring the first derivative of the wavefunction of the system to be discontinuous in each point where the Dirac delta has non-zero support. Far from this region, the system is described by a non-interacting theory.
To better understand this point, consider the eigenfunction of two generic particles at the positions x_1 and x_2 subjected to delta interaction and confined in a one-dimensional box of length L. The domain of the function is displayed in Fig. 2: we can see that the latter is divided into two subdomains $x_1 > x_2$ and $x_1 < x_2$ in which the delta interaction has no effect. As a consequence, in each of them, the wavefunction describes two free particles. These two sectors are separated by a boundary $x_1 = x_2$ on which the delta has non-zero support: in this sense, one can solve the Schroedinger equation of the interacting problem imposing additional boundary conditions on the free wavefunction in each sector and then using the superposition principle to obtain the more general solution. What we stated so far can be easily generalized to the case of N particles, provided that the sectors described by the free theory cover without overlapping the entire domain of the eigenfunction and the interactions only occur on the boundaries between each pair of subdomains.

Remarkably, since the N particles generalization of what we displayed so far involves the superposition of all the possible coordinate sectors, the general form of Bethe Ansatz wavefunction requires the summation of $N!$ terms, that represent all the possible permutations of the coordinates of the particles. This implies that Bethe Ansatz, due to the large number of terms in the eigenfunction also in few particles systems, doesn't provide a comfortable solution for models if one is interested in computing quantities that depend on the entire form of the wavefunction. Some examples of such calculations are density profiles or correlation functions. On the other hand, as we will see in the following chapters, this technique furnishes a very effective and rapid way to obtain observables such as the energy of the system and the momentum and thus will be particularly useful for this thesis.

In the first chapter, we provide a general introduction to the physics of ultracold atoms and to some experimental techniques used to trap and manipulate quantum gases. Then, we focus in particular on the realization and the application of one-dimensional systems, presenting more in detail some results concerning ultracold gases confined on a ring-shaped geometry. After a general discussion about this topic, we will restrict our analysis to experiments and physical properties of Fermi quantum gases.

In the following chapter, Bethe Ansatz is used to report the exact solution to the Schroedinger equation of a quantum Fermi gas subjected to attractive contact interaction and confined on a ring, *i.e.* the so-called attractive Gaudin-Yang model. In particular, considering the non-polarized case, that is same number of spin up and spin down particles, we examine the ground state of the model at any coupling regimes, from the weakly interacting state of paired fermions to the strongly attractive one, where the internal fermionic structure of the pairs can be totally neglected. This solution has been found independently by Gaudin[12] and Yang[13] in 1967. The main purposes of the chapter are to present Bethe Ansatz technique, that will be widely used in the following sections of the thesis, and to show a formal one-dimensional description of the BCS-BEC crossover. In the highly interacting regime of the model, a continuous evolution occurs between the quantum Fermi gas and a purely bosonic one, once some scaling transformations on the relevant parameters of the system are provided.
We will also display how that strict one-dimensionality of the model doesn't allow to reach the weakly interacting Bose-Einstein condensate regime since the interaction between the composite bosons results to be an infinite repulsion.

Then we study the attractive Gaudin-Yang model of rotating particles on a ring: exploiting the similarity between the formal expressions of Coriolis and Lorentz forces, we simulate the effect of a gauge field acting on a system of charged particles. Eventually, we obtain an exact expression for the energy of the ground state and of the persistent mass-current induced in the ring as a function of the angular velocity of the particles. In particular, we demonstrate the periodic behaviour of both quantities with respect to the latter. Remarkably, in analogy to what is obtained for persistent current of paired electrons in superconducting materials[14], such periodicity is halved if compared to the

one of the unbounded fermions. Another important result is that the period doesn't depend on the interaction strength and thus doesn't keep track of the different regimes of the crossover.

The last part of the thesis is dedicated to the description and to the study of the parity effect: a typical phenomenon that occurs in fermionic systems that concerns the dependence of some observables on the number of particles to be even or odd. In the case we are dealing with, such observables are the energy of the ground state due to the center of mass motion and the persistent current. We will see how for an odd number $N/2$ of paired fermions the application of the artificial gauge field makes the energy of the ground state to increase, driving the system in a less stable configuration: this behaviour is called diamagnetic, in analogy to what we have for magnetic fields acting on charged particles. On the contrary, if $N/2$ is even the artificial gauge field reduces the energy of the ground state, displaying a so-called paramagnetic behaviour.
The parity effect doesn't occur in bosonic systems since they always present a diamagnetic behaviour thus, according to the general theory, it must vanish in the high interacting bosonic limit of the model we are considering. As a consequence, we will numerically compute the exact form of the eigenfunction for the $N = 4$, thus an even number of pairs, and show how the system evolves from paramagnetic at low interactions to diamagnetic while the system is driven to higher values of the coupling constant. We will also compare the result with the exact and full solution of the two-particles problem obtained in Appendix B, where only the diamagnetic behaviour is observed.

Chapter 1

Ultracold atoms in one dimension: a general review

In the following, we will provide a review of the ultracold atoms gases confined in one dimension. First of all, we will present some experimental techniques implemented for the realization of such systems, discussing also the main theoretical differences with the usual three-dimensional systems. Afterwards, we will describe more in detail the applications of this kind of setups focusing in particular on Atomtronics experiments. We will include in the analysis both the most common bosonic systems and the more recent attempts to incorporate Fermi gases in this framework. Eventually, we will sketch some important features and results concerning ultracold fermionic systems that will be central in the following chapters of the thesis. In particular, we will present more in detail two important topics: the BCS-BEC crossover and its application in ultracold atoms and the Leggett theorem, which represents one of the most fundamental results concerning the persistent current in superconducting rings and more in general in fermionic systems.

1.1 1-D quantum systems: far more than toy models

Physical systems in one dimension represent nowadays a very rich source for theoretical and experimental research. Despite the great interest that such systems have occurred in science since more than one century, the great step forward for what concerns the physical relevance of one-dimensional models was made together with the first experimental realizations of these setups. Indeed the great progress in physics of materials and nanotechnology allows to realize, starting from the last decades of the XX century, several quasi one-dimensional structures such as Josephson junctions[15] arrays and ladder compounds[16]. At the beginning of the 2000s, the development of trapping techniques allows the creation and the manipulation of one-dimensional vapors of atoms. In the following, we will briefly describe some of the most common atom trapping protocols

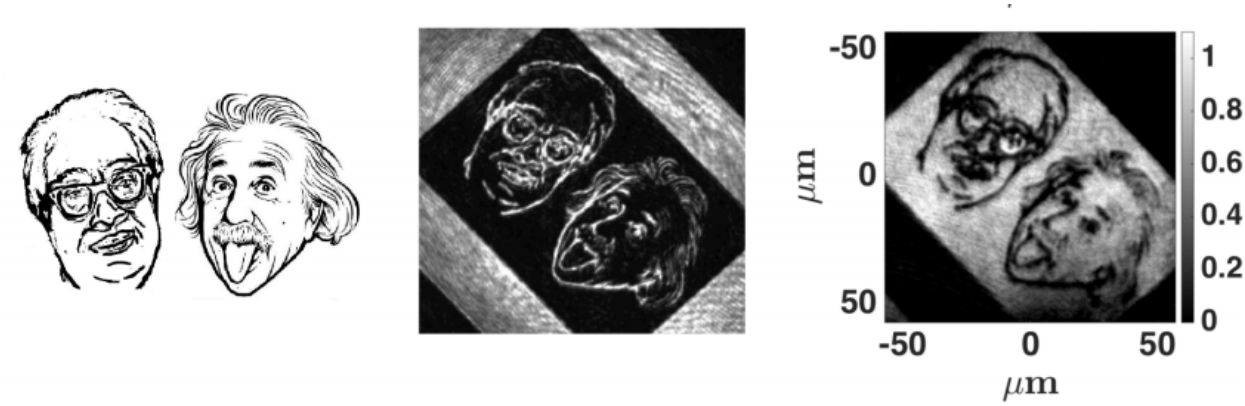

Figure 1.1: An image of Bose and Einstein realized with a condensate of $N = 5.2\ 10^5$ atoms averaged on 5 experimental runs. We can see the almost arbitrary manipulation of ultracold atoms provided by optical traps. Figure from [17].

useful for the realization of low dimensional quantum systems.

1.1.1 Optical trapping

This technique exploits the laser interference to confine the atoms in a given geometry[17]. The electric field generated by a laser beam induces a small dipole moment on the atoms that results in a confinement force proportional to the gradient of the field itself. In this way, the corresponding optical potential is proportional to the intensity of the light via a quantity called polarizability. The latter depends on the wavelength of the laser such that it is negative for blue detuned laser beams and positive if the light is red detuned.

Therefore, the region in which the atoms are confined can be modeled by the detuning from their resonant frequency and the intensity of the light[18]. A very common example of optical potential used in experiments is a standing wave potential propagating in one direction. One can produce a three-dimensional periodic lattice using a superposition of three waves and add a harmonic potential to obtain the one-dimensional confinement.

1.1.2 Magnetic trapping

This kind of trapping exploits the Zeeman coupling between atomic spins and an external magnetic field $\mathbf{B}$. The potential describing such interaction is:

$$V_{ZE} = -g\mu_B\ \mathbf{S}\cdot\mathbf{B}, \tag{1.1}$$

where g is the gyromagnetic ratio of the atoms, μ_B is the Bohr magneton and $\mathbf{S}$ is the spin of the atoms.

When the field is sufficiently homogeneous, the spins tend to align to the latter, being parallel or antiparallel. In the first case, the potential induced by this coupling has a

minimum when the field is very strong while in the second one the minima correspond to weak intensities of $\mathbf{B}$.

The most common way to implement such trapping techniques in a cigar-shaped geometry involves atoms chips: wires deposited on the surface of the trap generate the magnetic field. Most of these traps are built in order to have minima for weak field intensities. As a consequence, since the atoms must be coupled to a homogeneous weak field, the magnetic techniques usually implemented to tune the interactions of the system, known as Feshbach resonances, cannot be applied. However, it is possible to tune the coupling strength by changing the density (as discussed in Sec. 1.1.4 below) or using "confinement induced resonances" [19].

1.1.3 Conditions for one-dimensional regime

The trapping techniques described in Sec. 1.1.1 and Sec. 1.1.2 are very general and can be implemented to confine the system in a wide variety of different geometries. The question now naturally arises: how to obtain a strictly one-dimensional system? The key point is indeed to determine some parameters that fully specify the dimension in which we are confining the gas.

Once the quantum gas has been trapped in a 3-d potential, one can reach one-dimensional regime modulating the confinement in the two directions one wants to inhibit. For instance, consider a quantum gas confined in a three-dimensional harmonic potential. In this case, the frequencies of the oscillations along the three directions are very close to each other. If we want to confine the gas in a one-dimensional geometry, say along z direction, we can apply a two dimensional transverse potential in the directions x and y with a common oscillator frequency $\omega_\perp$. Assuming that the confinement energy $\hbar\omega_\perp$ is much higher than the energy scales of the one-dimensional system, we have that the excited transverse modes are cooled down: they are not accessible to the atoms. This is an example that shows how to obtain a strictly one-dimensional system starting from a three-dimensional confinement.

1.1.4 Dimensionless coupling constant

Defining a weak or strong interacting regime implies a coupling parameter that is independent of the unit of measurement. In order to build such a scale, we have to introduce the dimensionless coupling constant. Let's consider as particular case the contact potential, that represents one of the most common models for interactions in ultracold atoms physics. Such interaction depends on the spatial coordinates of the particles and it's non-vanishing only when two of these coincide, *i.e.* only if two atoms are placed in the same position. In the context of ultracold atoms it represents the Van der Waals force[20], a short-range interaction that is far weaker than the chemical bonds and that can be both attractive or repulsive. At low temperatures, only the s-wave atomic scattering is

relevant: within this assumption, the Van der Waals potential can be considered as a zero-range interaction. As a consequence, assuming an identical coupling among all the particles in the system, we can model this interaction using a Dirac delta distribution. Respectively in three and one dimensions, we will have the two potential terms for an N particles gas:

$$V_{3D} = g_{3D} \sum_{i \neq j}^{N} \delta(\mathbf{x_i} - \mathbf{x_j})$$
$$V_{1D} = g_{1D} \sum_{i \neq j}^{N} \delta(x_i - x_j), \tag{1.2}$$

where x_i represent the positions of the particles in the different three dimensional and one-dimensional real space.

Both potentials in (1.2) must have the physical dimensions of an energy. Applying a proper rescaling introducing a unit of mass μ and a factor $\hbar^2$ in order to express both the energy and the coupling constant in power of unit of length, dimensional analysis yields:

$$\left[\frac{\mu}{\hbar^2}\ g_{3D}\right] \equiv \Big[L\Big] \qquad\qquad \left[\frac{\mu}{\hbar^2}\ g_{1D}\right] \equiv \Big[L\Big]^{-1} \tag{1.3}$$

We can see from (1.3) that in order to obtain a dimensionless coupling constant we have to renormalize using a characteristic length. Introducing the densities n_{1D} and n_{3D} as the ratios between the number of particles and the volumes of the systems we obtain:

$$\gamma_{3D} = \frac{\mu}{\hbar^2}\ g_{3D}\ n_{3D}^{1/3}$$
$$\gamma_{1D} = \frac{\mu}{\hbar^2}\ g_{1D}\ n_{1D}^{-1} \tag{1.4}$$

As we previously recalled, these coupling constants define univocally the weak and the strong interacting regimes respectively in three and one dimensions. This relations allow to identify an highly significative difference between these two kind of physical systems relying on the density of the gas. Indeed in three dimensions the strong interacting regime occurs at high densities while in one-dimensional systems strong interactions are related to dilute gases.

1.2 Atomtronics: experimental techniques and state of art

An emergent research area of application for ultracold atoms is Atomtronics. As we have already delineated in the Introduction, this research area pursues the realization

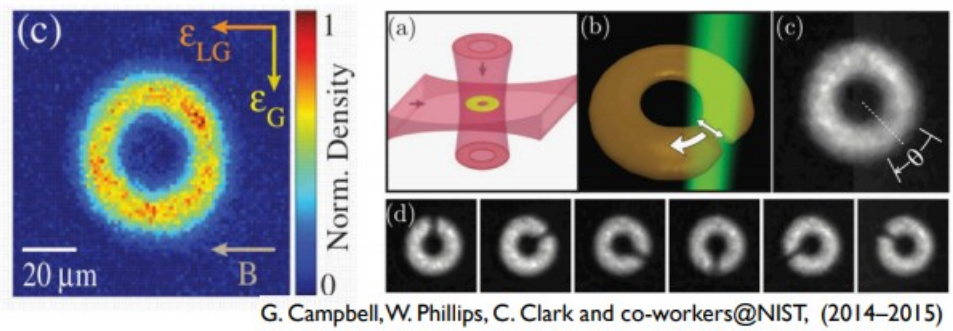

Figure 1.2: (a) A schematic picture of a toroidal optical trap for a Bose-Einstein condensate. (b) (c) and (d) show the toroidal trap with an additional rotating barrier on the ring, steering the atoms of the condensate. Figure from [22].

of analogs of electronics devices using atoms and molecules instead of charged particles. In this section, we will present some of the principal experimental results in this field, starting from the setups involving bosonic systems and then providing some outlooks about the use of Fermi gases.

Starting from the experiments in the context of ultracold atoms, thus the ones concerning the trapping of such systems in a desired geometry, one can exploit these setups to design devices useful for atomic circuitry or interferometry.

One of the most advanced experimental applications in the field is the realization of atomic transistors[21]. In these devices the trapping techniques are used to shape and manipulate the triple-well potential defining the three regions of an electronic transistor. In this case the electric current is substituted by a flow of atoms across the potential barriers and the current gain can be studied using the very same methods of the usual transistors. Another very interesting application concerns the realization of the analog of a superconducting quantum interferometer device (SQUID). This equivalence exploits the similarity between the eigenfunctions of a Bose- Einstein condensate and a superconductor. Moreover, both devices take advantage of the ring-shaped of the system in which they are confined. The flux through the ring can be simulated in the atomic system using a rotating barrier that steers the atoms.[22][23]

Consider a non-rotating Bose-Einstein condensate. Due to the ring geometry of the confinement potential, the wavefunction will be periodic and the angular momentum of the particles will be quantized. Breaking the rotational symmetry using a barrier, one can induce a transition in the momentum spectrum. Afterwards, the circulation can be detected by releasing the condensate from the trap and studying the time-of-flight distribution of the particles. Indeed, considering a non-rotating condensate, we have that a release from the ring-shaped trap would make the superfluid to collapse and to close the central hole almost instantaneously. On the contrary, a non-vanishing angular velocity would prevent this effect. As a consequence, measuring the time necessary for

the central hole to collapse, one obtains information about the rotation frequency with very high precision. From the analogy between the rotation of an atomic gas and the magnetic flux threading a ring of charged particles, delineated more in detail in Section 3.1, one can build the analogy between the device described so far and a superconducting interferometer.

1.2.1 Fermi gases in Atomtronics: present and future outlooks

All the experiments and applications described so far concern bosonic system and bosonic superfluids. In this section we will focus on Fermi ultracold gases and on some implementation of the latters. A crucial point for the applicability of Fermi gases is the fermionic superfluidity, that allows to exploit the same properties of a Bose-Einstein condensate in Atomtronics framework. This phenomenon is far more difficult to generate due to the Pauli principle that doesn't allow fermions of the same species to occupy the same state. As a consequence, at the heart of fermionic superfluidity, we have some pairing mechanism, that implies the formation of composite bosons reducing the influence of the Pauli exclusion and allowing a condensation process. The main theoretical protocols for pairing are the BCS theory of superconductivity and atomic-based phenomena like the BCS-BEC crossover, that will be both described in the following section.

It's worthy to notice that, conversely to Bose gases, fermionic superfluidity can only arise from interactions. This is one of the main reasons why such systems present a richer structure respect to a Bose condensate, in which the statistics of the particles is far more important to determine the phases of the gas and its properties.

The statistics of the particles also prevents to have superfluidity and in general contact interactions between spin-polarized Fermi gases. Consequently, in experiments it's fundamental to deal with different species of fermions that, in ultracold atoms framework, correspond to different hyperfine states of the atoms. Strong quantum degeneracy in fermionic systems has been observed at the end of the previous century in the group of JILA [24], where the low temperatures necessary for the superfluidity have been reached using a mixture two different species of fermions and bosons.

One of the main class of experiments for probing fermionic superfluidity concerns the so-called pairing-gap spectroscopy[25]. This technique requires a third level in the hyperfine structure that is not included in the pairing mechanism responsible for superfluidity. From a very general point of view, these experiments aim to probe the energy gap that underlines the formation of pairs, beyond which the latters are destroyed. To achieve this point, a radio-frequency field is applied to the gas, exciting only one component of the pair. In absence of a gap the resonant frequency of the transition would coincide with the energy difference between the excited and the ground level, assuming the system to be in the latter. An extra amount of energy to provide to the system in order to observe the transition, would display the presence of a gap and thus of pairs in the gas.

Future experimental outlooks concerning these systems aim a better understanding of

phenomena the unitary limit of the Fermi gases. This regime occurs when the scattering length of the system diverges and thus the latter becomes scale-invariant. In this limit the only relevant length is the interparticle distance, which is fixed by the density of the gas. Moreover, the superfluidity of mixtures of fermionic and bosonic particles can be studied[26], with the purpose of determining the proper mixtures of different species of fermionic atoms and bosons for which the entire gas is in a superfluid state.

In Atomtronics area of research, Fermi gases can be used to exploit some phenomena typical of this kind of systems to better characterize the pairing mechanism and the connection between superfluidity and superconductivity. An application in this sense would also be determining a protocol to better understand high-temperature superconductivity that goes beyond the phonon-mediated pairing occurring in low temperatures superconductors.

1.3 Ultracold Fermi gases: BCS-BEC crossover

In this section, we will describe in detail one of the most interesting phenomena occurring in quantum ultracold Fermi gases: the BCS-BEC crossover.

The better understanding of such behaviour of ultracold Fermi gases aims to provide a connection between the two separated worlds of superconductivity, which is the Bardeen Cooper Schrieffer pairing theory, and the superfluidity described by the Bose-Einstein condensation. First of all it's important to stress that BCS theory qualitatively describes a,lso some phenomena that go beyond the conventional superconductivity, as the pairing interactions of atomic nuclei[27] or the behaviour of some non-conventional p-wave superfluids[28]. A BCS-like state of N fermions can be briefly described as composed of $N/2$ paired fermions all in the same bound state whose size is larger than the interparticle spacing. Consequently, it is possible to picture such pairs in terms of a condensate of bosonic particles. The idea of a continuous crossover between these two regimes arouses in the 1960s and the three-dimensional qualitative phase diagram has been obtained before the experimental realizations using ultracold atoms.[29]

In order to explain the different phases of the crossover pictured in Fig 1.3, it is useful to introduce the scattering length a that univocally defines the scattering amplitude in the low energy limit. Considering a scattering process involving only s-waves we have:

$$\lim_{k\to 0} \sigma = 4\pi a^2, \tag{1.5}$$

where σ is the cross scattering section and k is the wave vector. In this framework, weak interactions are connected to a negative scattering length and the BCS regime is reached for $1/(k_f\, a) \to -\infty$, where k_f is the Fermi momentum and represents the inverse of the distance between the particles. Starting from this regime the scattering length can be tuned and brought to divergence: this limit is the so-called unitary limit of Fermi

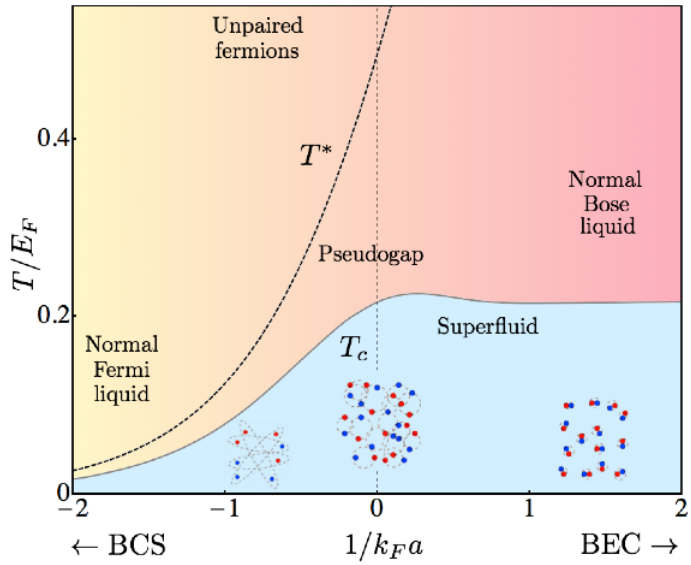

Figure 1.3: Phase diagram of the BCS-BEC crossover with respect to the scattering length a and the temperature. The evolution of the critical temperature all along the crossover is still an open problem: it can be determined experimentally in the different regimes. Fig.reproduced from [8].

gases. For strong attraction $a > 0$ and the BEC regime is reached when $1/(k_f\, a) \to +\infty$. Despite the Bose condensation is reached for high interaction, the formation of tightly bound dimers resolves in a weak interacting Bose gas in which the bound states repel each other for the residual effect of the Pauli principle. This counterintuitive feature can be understood by studying the four body Schrodinger equation, which yields an explicit result for the scattering length of dimer-dimer interaction that is reduced respect to the one of the initial model[9].

The experimental realization of BCS-BEC crossover relies on the possibility of tuning continuously the scattering length exploiting Feshbach resonances. From a very general point of view, this phenomenon occurs in a two-particle scattering when a bound state in a closed channel is coupled to the open channel of the process. This can be achieved by varying the energy of the closed channel using an external magnetic field that acts on the hyperfine states of the atom and induces a resonant condition. Such process produces a change of sign in the scattering length from negative to positive, thus from attractive to repulsive interactions. When the bound state crosses the threshold of the continuous state in the open channel, the scattering length diverges and the system is in the unitary limit where the system is scale-invariant and the only characteristic length is the interparticle spacing proportional to k_f^{-1}. As we have already anticipated in the Introduction, the strictly one-dimensional description of this phenomenon presents several differences from the usual three dimensional one. On one hand, the model of a Fermi gas subjected to attractive contact interaction is integrable and thus can be exactly

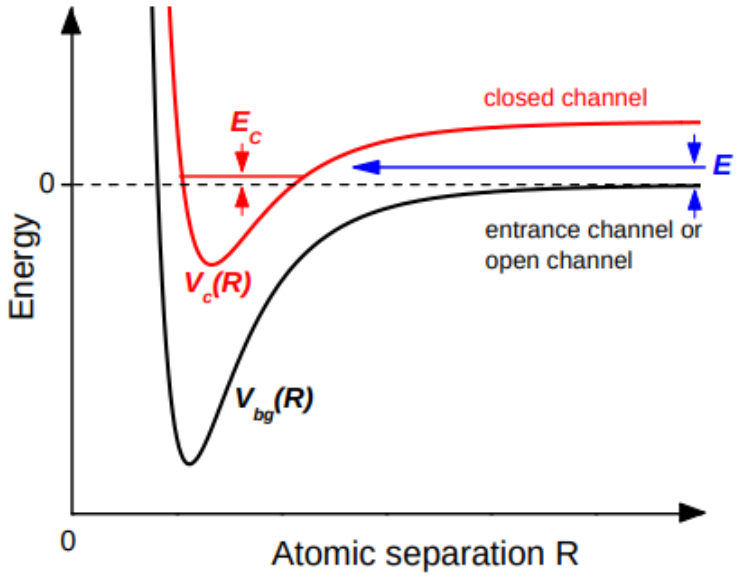

Figure 1.4: Schematic protocol of a Feshbach resonance: the external magnetic field acts on the hyperfine states of the atoms in order to induce a resonant condition between the energies E_c and E. This opens a bound state channel that a priori would have been far more unstable than the continuous one. Figure from [10].

solved at any interaction strength, on the other hand the bosonic limit of such model behaves like a Tonks-Girardeau gas of hardcore bosons (see Appendix 1) and one never reaches the weakly interacting Bose condensate. A future outlook for the present research could be to study the quasi-one-dimensional crossover, that is a three-dimensional model confined in a one-dimensional waveguide. In this case, as explained in reference [11], an analog of the 3D crossover can be achieved exploiting a confinement induced resonance that interprets the role of the three dimensional Feshbach resonance, inducing a coupling between an open and a closed channel in the trap and properly tuning the scattering length. In this limit, the weak interacting bosonic limit exists and the Bose condensation of the paired fermions occurs, although at the present moment there's no an experimental realization of such theoretical protocol in one dimension.

1.4 Persistent currents in electronic and atomic systems: the Leggett Theorem

Let's now introduce an important concept in the framework of physics in ring-shaped potentials, originally concerning a system of fermions in a superconductor but, as we will show in Chapter 3, also very relevant in the context of ultracold fermionic atoms.

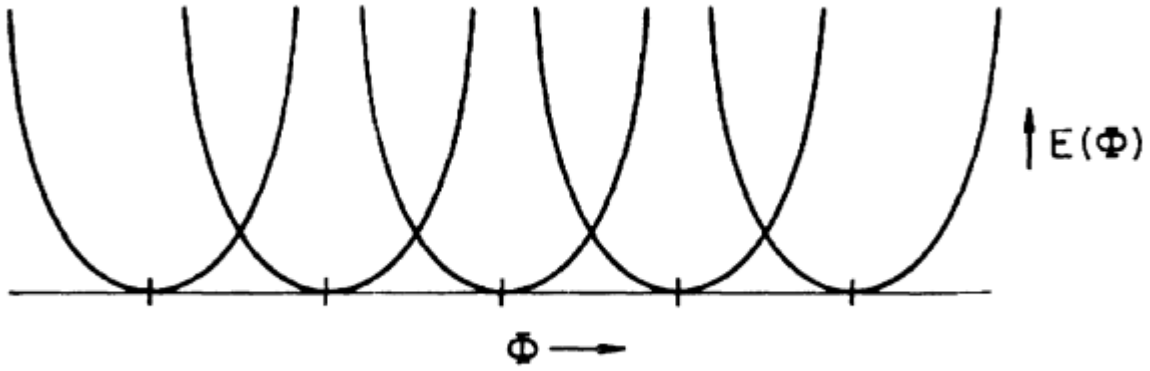

Fig. 4 The trivial band structure (V(θ) = 0).

Figure 1.5: We can see the energy of the electrons on the ring showing a periodicity with respect to the magnetic flux. Since the current is the derivative of the energy respect to the latter, the period will be the same. Figure from [31].

Consider a metallic ring and a magnetic flux passing through it. The periodicity of the eigenfunction required by the shape of the system can be twisted by a phase that takes into account the gauge transformation including the effect of the flux [30].

$$\Psi(\theta_1 = 0, \theta_2 ... \theta_N) = e^{i\Phi/\Phi_0}\Psi(\theta_1 = 2\pi, \theta_2 ... \theta_N), \tag{1.6}$$

where θ_i are the angular coordinate of the N particles on the ring and Φ is the magnetic flux through the ring. The quantity Φ_0 is called quantum of flux and for free electrons we have $\Phi_0 = h/e$ being e the elementary charge. In such framework a non-dissipative current, defined for zero temperature as the derivative of the energy with respect to the flux, is induced in the ring.

The very same phenomenon occurs in a superconducting ring, with the only difference that the quantum of flux results to be halved. This is coherent with the fact that the charge carriers in this case are paired fermions, that transport a charge of $2e$. A very general result relating the persistent current and the quantum of flux is both systems is the Leggett theorem [31]. Such theorem concerns systems of N fermions described by an Hamiltonian in the form:

$$H_{Legg} = \sum_{i=1}^{N} \frac{1}{2m}\Big(p_i - eA(\theta_i)\Big)^2 + \sum_{i=1}^{N} V(\theta_i) + \sum_{ij} U(\theta_i - \theta_j), \tag{1.7}$$

where A is the vector potential minimally coupled to the momenta of the particles, U is an arbitrary fermion-fermion interaction and V represent a term of local disorder. Given an Hamiltonian in this form, the theorem states two important results:

- The current is periodic with respect to the flux and the period coincides with the quantum of flux of the components of the system or with an integral function of the latter. Such period doesn't depend neither on interaction U nor on local disorder V.

- If we consider spinless fermions, the number of particles N defines the diamagnetic or paramagnetic behaviour of the material. Indeed if N is even we have that the energy of the system is maximum at $\Phi = 0$, while for odd values of N we have a minimum in $\Phi = 0$: the sign of the persistent current is different in the two cases.

The main features emerging from this theorem are the importance of the quantum of flux in describing the persistent current and the existence of parity effects in this framework. The first one states that once the current components are determined and thus the quantum of flux is fixed, apart from some pre-factor due to an integration, the behaviour of the persistent current with respect to the flux is univocally defined at any two-body interaction and at any level of local disorder. The second feature formalizes the present of parity effect, that will be studied in Chapter 4, relating the response of the material to the application of an external gauge field to the number of particles in the system. It's important to stress again that the second point of the previous list is valid for spinless electrons or equivalently for fully polarized fermions.

Such theorem was initially applied to electrons in a metal ring, but as we will see the great arbitrariness of the Hamiltonian makes it easily generalized to different kinds of fermions, including ultracold atoms. This is possible because the delta interaction, that is the common fermion-fermion coupling in ultracold atoms, is included in the ones appearing in the Hamiltonian (1.7). In the following we will simulate the action of a gauge field acting on charged particles on a system of neutral atoms: in order to check the accuracy of our treatment will be very important to compare our results with the Leggett theorem, stressing the similarities and properly explaining the differences.

Chapter 2

One-dimensional crossover: a Bethe Ansatz formal derivation

The first step to take to provide a theoretical description of a crossover between a fermionic and a bosonic model is to impose a one-to-one mapping between the formal expressions associated with the physical quantities that describe the system in the two cases. This will allow to properly fix the regime in which the two models can be legitimately considered equivalent and also to study the continuity of the process in order to make a distinction between a crossover and a phase transition. Since we are interested in studying the ground state of a one dimensional model of attractive Fermi gas and in investigating the limit in which interactions allow to describe the system using a bosonic model, the most relevant quantities we want to be equivalent are the energies of the respective ground states. Therefore, in the following, we will explicitly derive an identity originally underlined by Gaudin in the original Bethe Ansatz solution of the model of a Fermi gas with attractive delta interaction confined on a ring. This identity concerns the energy of the ground state of this model and the correspondent quantity in a one dimensional model of repulsive bosons with the same kind of interaction, the so-called repulsive Lieb-Liniger gas[32]. Indeed, once the thermodynamic limit is applied to both expressions, it's possible to perform a power series expansion in the respective strong interacting regime, *i.e* strong attractive fermions and strong repulsive bosons. This allows to obtain two identical expressions besides a change of sign in the corresponding dimensionless coupling constants and a proper rescaling of the mass and the density of the particles. Remarkably, in order to obtain the continuous crossover, the mass of the bosons must be double of the mass of the fermions, while the densities are in the inverse ratio. This is coherent with the physical picture of composite bosons made up by paired fermions in which the extreme tight bounds allow to neglect the internal degrees of freedom.
The first step in the derivation of the crossover will be to show the Bethe Ansatz exact solution for both Gaudin-Yang and Lieb-Liniger model. Afterwards, the formal mapping

between the energies of the ground state in the thermodynamic limit will be displayed by studying the strongly attracting and strongly repulsive regimes respectively for fermions and bosons.

2.1 Bethe Ansatz for Lieb-Liniger model

We start revising the Bethe Ansatz solution for the Lieb-Liniger model, following [32]. Let us consider the Schroedinger equation for N bosons in the interval $0 \leq x_i \leq L$ and subjected to a repulsive contact interactions:

$$\Big(-\frac{\hbar^2}{2m_B}\sum_{i=0}^{N}\frac{\partial^2}{\partial x_i^2} + g\sum_{i<j}\delta(x_i - x_j)\Big)\Phi(\mathbf{x}) = E\Phi(\mathbf{x}), \tag{2.1}$$

where $g > 0$ and $\mathbf{x} = (x_1, x_2 ... x_N)$ is the vector that specifies the positions of the N particles. Equation (2.1) can be expressed in an equivalent way through the system:

$$\begin{cases} \Big(-\frac{\hbar^2}{2m_B}\sum_{i=0}^{N}\frac{\partial^2}{\partial x_i^2}\Big)\Phi(\mathbf{x}) = E\Phi(\mathbf{x}) \\ \\ \Big(\frac{\partial}{\partial x_{j+1}} - \frac{\partial}{\partial x_j}\Big)\Phi(\mathbf{x})|_{x_{j+1}=x_j} = \frac{2m_B g}{\hbar^2}\Phi(\mathbf{x})|_{x_{j+1}=x_j} \end{cases} \tag{2.2}$$

Imposing periodic boundary conditions (PBC) for all the coordinates of the N particles $x_i, \forall i = 1...N$:

$$\Phi(0, x_2, ...x_N) = \Phi(x_2, ...x_N, L) \tag{2.3}$$

we may solve Eq.(2.2) using the Bethe Ansatz:

$$\Phi(\mathbf{x}) = \sum_{\mathsf{P}} B(\mathsf{P}) \exp\Big\{i\sum_{j=1}^{N} k_{\mathsf{P}(j)} x_j\Big\}, \tag{2.4}$$

where the summation is performed over all the permutations P of N rapidities k_j. From the first of equations (2.2) one has that the energy eigenvalues are given by:

$$E_B = \sum_{j=1}^{N}\frac{\hbar^2 k_j^2}{2m_B} \tag{2.5}$$

while the second equation fixes the coefficients $B(\mathsf{P})$. Indeed consider two permutations P and Q such that:

$$k_{P(1)} = k_{Q(2)}, \quad k_{P(2)} = k_{Q(1)}$$

By assuming linear independence of the addenda in the sum (2.4) we can substitute in (2.2) only the terms regarding these two permutations. One obtains the following relationships between the coefficients:

$$B(Q) = -B(P)\frac{\frac{2m_B g}{\hbar^2} - ik_{P(2)} + ik_{P(1)}}{\frac{2m_B g}{\hbar^2} + ik_{P(2)} - ik_{P(1)}} \equiv -B(P)e^{i\theta(k_2-k_1)} \tag{2.6}$$

Considering all the different pairs of permutations, we will have analogous relations. In order to fix properly all the coefficients, we can start from a value $B(\mathbb{1}) = 1$ and then decompose each permutation P in transpositions, building the phase defining $B(\mathsf{P})$ by simply composing the phases relative to each transposition. Explictly, for a generic permutation P we have:

$$B(P) = \prod_{\mathbf{T_{ij}}} -e^{i\theta(k_i-k_j)} \tag{2.7}$$

Where $\mathbf{T_{ij}}$ constitutes a sequence of transpositions involving the rapidities k_i and k_j in which P can be decomposed.

In order to determine the precise form of the allowed rapidities k_j we have to apply the PBC: a substitution of Bethe Ansatz wave function (2.4) in equation (2.3) yields:

$$(-1)^{N-1}\exp\Big\{i\sum_{i=1}^{N}\theta(k_i-k_j)\Big\} = \exp\Big\{-ik_jL\Big\} \tag{2.8}$$

This relations holds for all k_j: taking the product of all these equations and noting that $\theta(k_i - k_j) = -\theta(k_j - k_i)$ one eventually has:

$$\sum_{j=1}^{N} k_j = \frac{2\pi m}{L} \quad m \in \mathbb{Z} \tag{2.9}$$

that implies that the center of mass momentum doesn't depend on interactions and take any multiple value of $\frac{2\pi}{L}$. Relation (2.9) brings to the quantization of the total momentum of the particles, whose expression can be computed directly from Schroedinger equation:

$$\hat{P}\Phi(\mathbf{x}) = -i\hbar\sum_{j=1}^{N}\frac{\partial\Phi}{\partial x_j} = \Big(\sum_{j=1}^{N}\hbar k_j\Big)\Phi(\mathbf{x}) \tag{2.10}$$

Notice that we have assumed the rapidities to be real in this case, since there are no bound states for repulsive bosons. Taking the logarithm of Eq.(2.8) we obtain the following equation for the rapidities:

$$k_jL = -\sum_{s=1}^{N}\theta(k_s-k_j) + 2\pi m_j, \tag{2.11}$$

where m_j are integers or semintegers depending on the number N of bosons being odd or even respectively.

2.1.1 Thermodynamic limit and ground state

Consider the limits $N \to \infty$ and $L \to \infty$, provided $n_B \equiv N/L$ finite and fixed. We identify the ground state of the system fixing the minimum distance between the k_js. Introducing a density of rapidities:

$$f_B(k_j) = \frac{1}{(k_{j+1} - k_j)L} \tag{2.12}$$

one can eventually obtain the continuum limit using equation (2.11):

$$2\pi f_B(k) = 1 + \frac{4m_B g}{\hbar} \int_{-K}^{K} \frac{f_B(p)}{(\frac{2m_B g}{\hbar^2})^2 + (p-k)^2} dp \tag{2.13}$$

where the integral kernel comes from the expansion of the difference quotient of the Bethe phases and where the formal relation:

$$\frac{1}{L} \sum_s (...) = \int (...) f_B(p) dp$$

it's been used. The cut-off rapidity K is fixed by the request of normalization for the density of rapidities:

$$\int_{-K}^{K} f_B(x) dx = n_B \tag{2.14}$$

while the energy for unit of length of the ground state can be computed by taking the continuous limit in equation (2.5):

$$\frac{E_B}{L} = \frac{\hbar^2}{2m_B} \int_{-K}^{K} f_B(p) p^2 dp \tag{2.15}$$

Introducing the dimensionless coupling constant $\gamma_B = \frac{2m_B g}{\hbar^2 n_B}$ one may recast equation (2.13) in a suitable way:

$$2\pi f_B(k) = 1 + 2\gamma_B \int_{-K}^{K} \frac{f_B(p)}{n_B \left(\gamma_B^2 + \frac{1}{n_B^2}(p-k)^2 \right)} dp \tag{2.16}$$

Hence, to obtain the exact ground-state energy E_B at any interaction strength, one has first to obtain the density of rapidities from the equation (2.16) and then insert it in Eq. (2.15).

2.2 Bethe Ansatz for Gaudin-Yang model

We next revise the Bethe Ansatz solution for the Gaudin Yang model [12]. Consider now a system of $N = N_\uparrow + N_\downarrow$ attracting fermions of mass m_F confined in a spatial region of dimension L, where the arrows refer to the spin degree of freedom. Considering the non-polarized case, we can set $N_\uparrow = N_\downarrow = N/2$ and assuming that the interaction can be described by a δ-potential, we have a Schroedinger equation similar to (2.1):

$$\Big(-\frac{\hbar^2}{2m_F}\sum_{i=0}^{N}\frac{\partial^2}{\partial x_i^2} + c\sum_{i<j}\delta(x_i - x_j)\Big)\Psi(\mathbf{x}) = E\Psi(\mathbf{x}), \tag{2.17}$$

where in this case $c < 0$. As in the bosonic case we can decouple this equation in a system analogous to (2.2) and require that the system satisfies the PBC (2.3). In the following, a Bethe Ansatz solution is investigated:

$$\Psi(\mathbf{x}) = \sum_{\mathsf{P}} A(\mathsf{P})\exp\Big\{i\sum_{j=1}^{N} q_{\mathsf{P}(j)}x_j\Big\} \tag{2.18}$$

The coefficients $A(P)$ are fixed by requiring discontinuity in the first derivative of the eigenfunction in all the points in which delta-interactions between two particles with antiparallel spins occur. Proceeding as in the previous section, one obtains an equation for the Bethe phases and coefficients:

$$A(P) = -\prod_{\mathbf{T_{ij}}} e^{i\phi(q_i - q_j)}, \quad A(\mathbb{1}) = 1 \tag{2.19}$$

$$e^{i\phi(q_k - q_j)} = \frac{\frac{2m_F c}{\hbar^2} - iq_k + iq_j}{\frac{2m_F c}{\hbar^2} + iq_k - iq_j} \tag{2.20}$$

The main difference between bosonic and fermionic systems relies on the symmetries of the coefficients $A(P)$. Indeed, each time a permutation involves a transposition between rapidities associated to particles with the same spin, a factor (-1) must be applied to (2.19) in order to preserve the antisimmetry properties of the eigenfunction. As a consequence, imposing PBC yields a slightly different expression for allowed rapidities:

$$\exp\{-iq_jL\} = \prod_{s=1}^{N/2}\exp\{i\phi(q_s - q_j)\} \tag{2.21}$$

String Hypothesis

Since we are dealing with attractive interactions, we have to take into account the formation of bound states in the lowest energy level. Such paired fermions will be described

assuming the so-called string hypothesis, with the additional constraint for the number of particle N to be even: in view of thermodynamic limit this can be assumed without any loss of generality.
The string hypothesis relies on the fact that the rapidities defined in (2.21) assume the following form:

$$\tilde{q_j}^{\pm} = u_j \pm iv_j, \quad j = 1..N/2, \quad u_j, v_j \in \mathbb{R} \; \forall \; j \tag{2.22}$$

It's worthy to notice that this formalism requires the rapidities to be pairwise complex conjugated to constrain the expression of the energy analogous to (2.5) to assume only real values. In order to fix the imaginary part v, consider equation (2.21): after using (2.22) one obtains that in thermodynamic limit the left-hand side either diverges to infinity or goes to zero, depending on the sign of the imaginary part. As a consequence, in order to have a pole or a zero on the right-hand side, we have that each rapidity must have an imaginary part in the form $v_j = v = \pm\frac{m_F}{\hbar}c$.

Taking the logarithm of Eq.(2.21) we obtain:

$$q_j L = -\sum_{s=1}^{N/2} \phi(q_s - q_j) + 2\pi r_j, \tag{2.23}$$

where $r_j \in \mathbb{Z}$. The energy eigenvalues can be expressed by:

$$E_F = -\frac{N\hbar^2(c/2)^2}{2m_F} + \sum_{j=1}^{N/2} \frac{\hbar^2 u_j^2}{2m_F} \equiv -N|\epsilon_b| + E_F^{eff} \tag{2.24}$$

where the first term represents the bound energy of the pairs.

2.2.1 Thermodynamic limit and ground state

Let's now focus on the study of the ground state properties in thermodynamic limit $(N, L) \to \infty$ keeping finite the fermion density $n_F = N/L$. Defining the density of pairs rapidities as:

$$f_F(q_j) = \frac{1}{(q_{j+1} - q_j)L} \tag{2.25}$$

and proceeding as for the Lieb-Liniger model, one obtains from (2.23):

$$2\pi f_F(q) = 2 + \frac{4m_F c}{\hbar^2} \int_{-Q}^{Q} \frac{f_F(p)}{(\frac{2m_F c}{\hbar^2})^2 + (p-q)^2} dp, \tag{2.26}$$

where the normalization constraint reads:

$$\int_{-Q}^{Q} f_F(x)dx = \frac{n_F}{2} \tag{2.27}$$

As a consequence, from (2.24) we have that the effective energy for unit of lenght of the ground state is:

$$\frac{E_F^{eff}}{L} = \frac{\hbar^2}{2m_F}\int_{-Q}^{Q} f_F(p)p^2 dp \tag{2.28}$$

where the bound energy of the pairs has been incorporated in the first member.

Equation (2.26) can be expressed as well in terms of a positive adimensional coupling constant $\gamma_F = -\frac{2m_F c}{\hbar^2 n_F}$:

$$2\pi f_F(q) = 2 - 2\gamma_F \int_{-Q}^{Q} \frac{f_F(p)}{n_F(\gamma_F^2 + \frac{1}{n_F^2}(p-q)^2)} dp \tag{2.29}$$

2.3 Analysis of the crossover regime

We now focus on the strongly interacting limit of Lieb-Liniger and Gaudin-Yang models *i.e.* the limit of highly attractive fermions and strongly repulsive bosons. Recalling the integral equations for rapidities densities:

$$2\pi f_B(k) = 1 + \frac{4m_B g}{\hbar^2}\int_{-K}^{K} \frac{f_B(p)}{(\frac{2m_B g}{\hbar})^2 + (p-k)^2} dp$$
$$2\pi f_F(q) = 2 + \frac{4m_F c}{\hbar^2}\int_{-Q}^{Q} \frac{f_F(p)}{(\frac{2m_F c}{\hbar^2})^2 + (p-q)^2} dp$$

we want to determine the relation between the coupling constants c and g under which a continuous crossover between these two regimes of the fermionic and bosonic model occurs. We follow the procedure adopted in Ref.[33]:

- The rapidities densities of both models will be expanded in power series and the correponding integral equations will be reduced to polynomial relations up to a finite order of the coupling constants;
- The explicit solutions of rapidities densities will be computed in the strongly interacting regimes of both models and will be used to obtain the energies of the ground states;
- Comparing the expressions of the energies, we determine the conditions under which a continuous mapping between two spectra can be performed.

We consider first the Gaudin-Yang density of rapidities: introducing the scale transformations:

$$\lambda_F = \frac{-2m_F c}{Q\hbar^2}, \quad x = q/Q, \quad y = p/Q, \quad f_F(Qx) = F_F(x), \tag{2.30}$$

the integral equation can be recast in the following form:

$$2\pi F_F(x) + 2\lambda_F \int_{-1}^{1} \frac{F_F(y)}{\lambda_F^2 + (y-x)^2} dy = 2 \tag{2.31}$$

Now, exploiting the symmetry of $F_F(x)$ respect to a change of sign in his argument, it is possible to expand such function in even power series:

$$F_F(x) = \sum_{n=0}^{\infty} a_n x^{2n} \tag{2.32}$$

In addition, the integral kernel of the equation can be expanded as well:

$$\frac{1}{\lambda_F^2 + (x-y)^2} = 2\lambda_F \sum_{n=0}^{\infty}\sum_{k=0}^{\infty}\sum_{l=0}^{\infty}\sum_{m=1}^{[(k-l)/2]+n} a_n \binom{k}{l} (-1)^{l+k+m-1}\ 2^{k-l}\ \frac{x^{k+l}}{k!} \times$$
$$\times \frac{\partial^k}{\partial(\lambda_F^2)^k}\left(2\lambda_F^{k-l+2n-1}\left(\lambda_F^{-2(m+1)}\frac{1}{2m} - \tan^{-1}(1/\lambda_F)\right)\right) \tag{2.33}$$

where $[x]$ is the floor function of x.
In order to obtain an expression for the coefficients a_n one must equate the terms at the same power in x. Since we are interested in the strong coupling limit, only the first two coefficients a_0 and a_1 will be taken into consideration so that $F_F(x) = a_0 + a_1\ x^2$. From Eq.(2.28) it's immediate to derive the rescaled version for the effective energy:

$$\frac{E_F^{eff}}{L} = \frac{\hbar^2\ Q^3}{2m_F} \int_{-1}^{1} F_F(x) x^2 dx \tag{2.34}$$

In order to obtain an expression independent from the cut-off rapidity Q, we can express the latter as a function of fermionic density, solving the normalization constraint:

$$Q \int_{-1}^{1} F_F(x) dx = \frac{n_F}{2} \tag{2.35}$$

Thus, as a function of the adimensional coupling constant γ_F the energy can be written as:

$$\frac{E_F^{eff}}{L} = \frac{\hbar^2 n_F^3}{2m_F}\frac{\pi^2}{12}\left(\frac{2\gamma_F}{2\gamma_F+1}\right)^2\left(1 + \frac{4\pi^5}{15(2\gamma_F+1)^3}\right) \tag{2.36}$$

An analogous procedure can be accomplished on the bosonic rapidities density. Indeed, by implementing the scale trasformation:

$$\lambda_B = \frac{2m_B g}{K\hbar^2}, \quad z = k/K, \quad t = p/K, \quad f_B(Kz) = F_B(z) \tag{2.37}$$

one obtains the integral equation:

$$2\pi F_B(z) - 2\lambda_B \int_{-1}^{1} \frac{F_B(t)}{\lambda_B^2 + (t-z)^2} dt = 1 \tag{2.38}$$

The same expansion carried out so far yields the following expression for the ground state energy of Lieb-Liniger gas in the strong coupling limit:

$$\frac{E_B}{L} = \frac{\hbar^2 n_B^3}{2m_B} \frac{\pi^2}{3} \Big(\frac{\gamma_B}{\gamma_B + 2} \Big)^2 \Big(1 + \frac{32\pi^5}{15(\gamma_B + 2)} \Big) \tag{2.39}$$

It is now immediate to verify that, upon the transformations:

$$n_F = 2n_B, \; m_F = 1/2 \; m_B \rightarrow \gamma_B = 4\gamma_F \tag{2.40}$$

equation (2.36) and (2.39) assume the very same form providing a mapping between the ground-state energies of Gaudin-Yang attractive model and Lieb-Linger repulsive model in the strong coupling limit. From the non-singularity of such expressions in the limit $\frac{1}{\gamma_{F/B}} \rightarrow 0$ we can also state that the mapping is continuous. In conclusion, this analysis shows that in the limit of strong attractions the fermionic model tends to the one of bosonic point-like particles with strongly repulsive interactions.
It's worthy to notice that what we found so far implies that the crossover between the two models occurs in a regime in which paired fermions can be considered point-like particles up to the third order in the adimensional inverse coupling constant $1/\gamma_{B/F}$. A very interesting outlook for the future would be is to study at which order the two models deviate, and where the internal structure of the fermionic pairs starts to play a role.

Chapter 3

Artificial gauge field: a Bethe Ansatz analysis of persistent current

In the previous chapter, we have identified the precise interaction regimes that allow us to distinguish among fermions, composite bosons and point-like bosons in the model we are considering. In the following, after introducing the technique implemented to simulate the coupling with a magnetic field on charged particles, we use the Bethe Ansatz to provide an exact solution to the model presented so far taking into account the presence of an external artificial gauge field and a finite ring. The mesoscopic dimension of the system will enlight the presence of purely quantum effects in the ground state, such as non-zero persistent currents inside the ring that present a periodicity with respect to the elementary quantum of artificial gauge flux of the particles. In addition, we will show that such periodicity, in analogy with a system of electrons on a superconducting ring, is halved in the case of attractive fermions if compared to the non-interacting theory, coherently with the formation of pairs. Moreover, assuming a complete decoupling of Bethe wavefunction in center of mass and relative components, we show that the periodicity does not depend on the interaction strength: it retains the same value for each value of the coupling constant. This is because only the center of mass coordinate of the wavefunction is non-trivially affected by the artificial gauge field, while the contact interaction only influences the relative motion of the particles.

Since this phenomenon also regards bosonic systems, it will be also studied in the BEC regime. Despite the results presented in Appendix A on a gas of hardcore bosons show that the periodicity of the current is the same as a system of non-interacting fermions, the scaling transformations necessary to obtain a continuous crossover allow to recover the explicit value of the period for paired fermions. This is coherent with the independence of the period from interactions and shows that this quantity doesn't keep track of the different regimes of the BCS-BEC crossover.

3.1 Hamiltonian minimal coupling with artificial gauge field

In order to introduce an artificial gauge field acting on a quantum gas confined on a ring of radius R, we can induce a rotation of angular velocity Ω on the system, exploiting the similarity between the formal expressions of Coriolis and Lorentz forces. Suppose that the ring lies on the X-Y plane: the position of the i-th particle is specified by the arch $R\varphi_i$, where φ_i is the azimuth angle on the ring itself. Assuming a contact interaction between particles, the Hamiltonian of the system at rest can be written as:

$$H = -\sum_{i=1}^{N} \frac{\hbar^2}{2mR^2} \frac{\partial^2}{\partial \varphi_i^2} + \frac{g}{R} \sum_{i \neq j}^{N} \delta(\varphi_i - \varphi_j) \tag{3.1}$$

where g is an arbitrary real interaction constant. Performing the rotation described above around $\hat{Z}$ axis leads to a term that in cartesian coordinates reads:

$$-\Omega \hat{L_Z} = i\hbar \Big(\hat{Y} \frac{\partial}{\partial X} - \hat{X} \frac{\partial}{\partial Y} \Big) \tag{3.2}$$

to be added in the Hamiltonian. The transformation law:

$$\begin{cases} X = R\cos(\varphi) \\ Y = R\sin(\varphi) \end{cases} \tag{3.3}$$

allows to rewrite (3.2) respect to φ:

$$-\Omega \hat{L_Z} = i\hbar\Omega \frac{\partial}{\partial \varphi} \tag{3.4}$$

The Hamiltonian of the rotating system is:

$$\begin{aligned} H &= \sum_{i=1}^{N} -\frac{\hbar^2}{2mR^2} \frac{\partial^2}{\partial \varphi_i^2} + \frac{g}{R} \sum_{i \neq j}^{N} \delta(\varphi_i - \varphi_j) + i\hbar\Omega \sum_{i=1}^{N} \frac{\partial}{\partial \varphi_i} = \\ &= \sum_{i=1}^{N} \frac{1}{2m} \Big(\frac{-i\hbar}{R} \frac{\partial}{\partial \varphi_i} - m\Omega R \Big)^2 + \frac{g}{R} \sum_{i \neq j}^{N} \delta(\varphi_i - \varphi_j) - \frac{1}{2} m\Omega^2 R^2 \end{aligned} \tag{3.5}$$

We can see that rotation induces a shift in the momentum operator and in the potential energy in analogy with the minimal coupling to an elettromagnetic field: in this sense rotation can be intended as a proper model of a gauge field interacting with the system. In this analogy, the quantity Ω is called artificial gauge flux or *Coriolis* flux.

It's now immediate to map the ring in an one-dimensional interval of lenght $L = 2\pi R$, in which periodic boundary conditions allow to linearize the position of the particles imposing $x_i = R\varphi_i$. We obtain the 1D Hamiltonian:

$$\sum_{i=1}^{N} \frac{1}{2m}\Big(-i\hbar\frac{\partial}{\partial x_i} - m\Omega R\Big)^2 + g\sum_{i\neq j}^{N}\delta(x_i - x_j) + E_\Omega, \tag{3.6}$$

where we set $E_\Omega = -1/2\ Nm\Omega^2R^2$.

3.2 Gaudin-Yang model coupled with artificial gauge field

Let's now apply the Bethe Ansatz formalism developed so far to a one dimensional gas of N attractive fermions of mass m_F: we will refer to the Hamiltonian (3.6), imposing that $g = c < 0$ and $E_\Omega^{(F)} = -1/2\ Nm_F\Omega^2R^2$.
In analogy to what we did in the previous chapter, once defined $\mathbf{x} = (x_1...x_N)$ as the vector of the positions of the particles, we impose the Ansatz:

$$\Psi(\mathbf{x}) = \sum_{\mathsf{P}} A(\mathsf{P})\exp\Big\{i\sum_{j=1}^{N} q_{\mathsf{P}(j)}x_j\Big\},$$

where q_j represent the distinct rapidities of the particles. It's worthy to notice that the coupling with the artificial gauge field can be equivalently expressed shifting the rapidities q_j or even modifying the periodic boundary conditions through the application of a twisting phase by implementing a gauge transformation on (3.6). Since all these formulations are equivalent in order to preserve the gauge invariance, in the following we will write the explicit coupling term in the Hamiltonian, leaving the formal expression of the eigenfunction unaffected by the field.
In addition, we note that the discontinuity on the first derivative of Ψ due to the delta-interaction is not affected by the coupling with the artificial gauge field once the continuity of wavefunction is assured. From this last conclusion, we can infer that the expression for the Bethe coefficients is the same as the theory at rest reported in (2.19) and (2.20).

Let's now apply the periodic boundary conditions that must hold $\forall x_i \in [0, L]$:

$$\Psi(0, x_2...x_N) = \Psi(x_2, ...x_N, L).$$

Substituting the wavefunction in this relation one obtains $\forall j = 1...N$:

$$\exp\{-iq_jL\} = \exp\{i\sum_{s=1}^{N}\phi(q_s - q_j)\}, \tag{3.7}$$

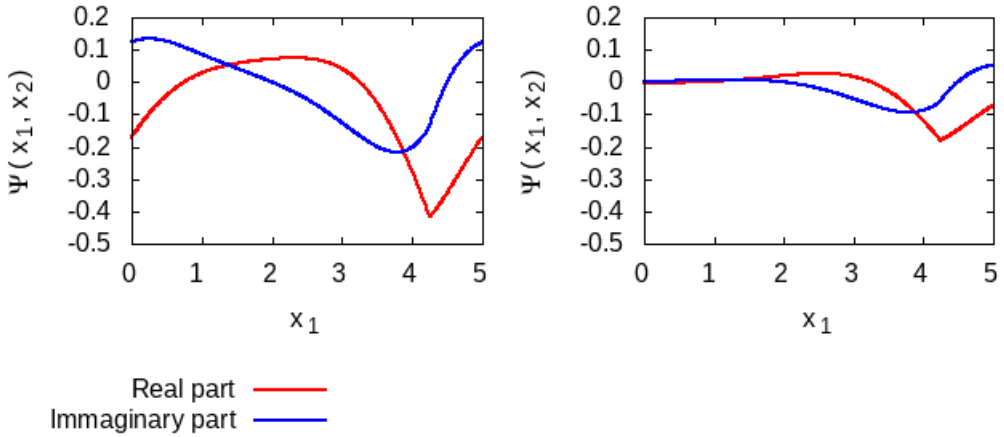

Figure 3.1: Comparison between real and imaginary part of the eigenfunction for $N = 2$ and coupling constant $2m_F c/\hbar^2 = -2$ evaluated using string hypothesis (right) and using exact solution of (3.8)(left). The position of the second particle is fixed at $x_2 = 4.25\ l$ on a total lenght of the system $L = 5\ l$, with l unit of length.

from which we can derive the explicit expression for the fermonic rapidities:

$$q_j = -\frac{1}{L}\sum_{s=1}^{N}\phi(q_s - q_j) + \frac{2\pi}{L}n_j, \quad n_j \in \mathbb{Z} \tag{3.8}$$

As we did in the previous chapter, we will make some assumptions about the expression of the rapidities related to the bound states. In analogy to what we have done for the infinite system, we will consider complex-valued rapidities, two by two conjugated in order to assure the energy eigenvalues to be real. On the other hand, since we are considering a finite system, we may expect that the imaginary part of such rapidities will present some deviations from the value of $\pm\frac{m_F c}{\hbar}$ fixed in $L \to \infty$ limit that follows from the application of the string hypothesis. What we stated so far is well displayed in Fig.3.1 and Fig.3.2 as obtained from the solution of the $N = 2$ exact equations (see Appendix B for details). We can observe that the periodicity of the eigenfunction is assured on the boundary of the system only considering the exact solution for finite values of L. Indeed, a straightforward substitution in the eigenfunction of rapidities whose imaginary part is the one obtained from the string hypothesis doesn't take into account the edge effects due to the decay of the eigenfunction when the second particle is placed very close to the boundary. This is our first important result: the string hypothesis does not ensure the correct periodicity of the wavefunction on the finite ring.

In the following, we want to determine the dependence of the ground state energy on the Coriolis flux Ω. For this purpose, exploiting the fact that in a homogeneous system center of mass and relative coordinate decouple, we separate the energy eigenvalues of

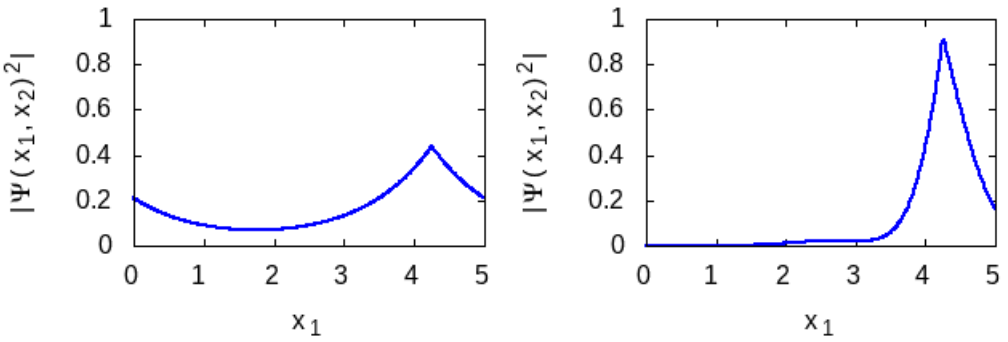

Figure 3.2: Modulus square of the eigenfunction, as a function of the coordinate x_1 for $x_2 = 4.25$ l, in the same case considered in Fig.3.1. From this plot we can see that the spatial density of the state present a peak when the two fermions are close to each other. If the fixed particle is placed sufficiently close to the boundary, in string hypothesis framework the eigenfunction doesn't keep track of the periodicity of the system.

the system in two different terms related to the formation of the bound states and to an effective positive contribution. In order to achieve this, one can introduce the center of mass and the Jacobi relative coordinates[34]:

$$\begin{cases} r^{com} = \frac{1}{N}\sum_{k=1}^{N} x_k \\ \\ r_j^{rel} = \left(\frac{j}{j+1}\right)^{1/2}\left(\frac{\sum_{k=1}^{j} x_k}{j} - x_{j+1}\right) \end{cases} \tag{3.9}$$

In this frame of coordinates the Hamiltonian (3.6) can be recast as:

$$H = \frac{1}{2Nm_F}\Big(P_{com} - m_F\Omega R\Big)^2 + \sum_{l=1}^{N-1}\frac{Q_l^2}{2m_F} + E_\Omega^F, \tag{3.10}$$

where it is important to stress again that the contact interaction term has not been included because it can be equivalently treated as a discontinuity condition to be imposed on the eigenfunction: it does not explicitly appear in the Schroedinger equation. The conjugate momentum operators that appear in the Hamiltonian are obtained by imposing canonical commutation relations with the corresponding coordinates. Explicitly, they assume the following form:

$$P_{com} = -i\hbar\sum_{j=1}^{N}\frac{\partial}{\partial x_j} \tag{3.11}$$

$$Q_l = \frac{-i\hbar}{\sqrt{l(l+1)}}\left(\sum_{p=1}^{l}\frac{\partial}{\partial x_p} - l\frac{\partial}{\partial x_{l+1}}\right) \tag{3.12}$$

It is important to observe from (3.10) that the dependence of the energy of the system on Ω induces a shift in the centre of mass momentum: the rotation does not influence the contribution to the energy provided by the relative motion.

One may now solve the Schroedinger equation for Hamiltonian (3.10) by a straightforward application of (3.12) and (3.11) to Bethe wavefunction. The energy eigenvalues will be expressed as a function of the rapidities related to the new coordinates:

$$E_F = \frac{\hbar^2}{2Nm_F}\Big(q_{com} - m_F\Omega R\Big)^2 + \sum_{l=1}^{N-1}\frac{\hbar^2}{2\mu_F}(q_l^{rel})^2 + E_\Omega^F, \tag{3.13}$$

where μ_F is the reduced mass of the fermions. The rapidities q_{com} and q_l^{rel} are respectively associated to the center of mass and to the l-th relative coordinate and have been defined as:

$$q_{com} = \sum_{j=1}^{N} q_j \tag{3.14}$$

$$q_l^{rel} = \frac{1}{\sqrt{l(l+1)}}\Big(\sum_{p=1}^{l} q_p - l\ q_{l+1}\Big) = \frac{1}{\sqrt{l(l+1)}}\Big(\sum_{p=1}^{l} p\ (q_p - q_{p+1})\Big) \tag{3.15}$$

In the following, we want to study how the energy of the ground state of the system varies with respect to the rotation frequency Ω. In order to do this, the first step is to characterize the ground state fixing the quantum numbers n_j labeling the rapidities of the particles such that the corresponding energy is minimum. It should be noted that to obtain the ground state of the system it is sufficient to minimize the first term in (3.13) because, as we have previously noticed, the relative momenta will be not affected by the transitions induced by the rotation of the particles.
We assume the following conditions:

- In the ground state the real parts of the rapidities of the pairs are reciprocally as close as possible;
- We introduce an integer $\bar{n} = n_1$ that labels the lowest energy level and must be fixed to the value that minimizes the modulus of the summation of the rapidities: such value will explicitly depend on N.

Let's now focus on how to characterize excitations in the system of the center of mass and relative coordinates. First of all, for sake of simplicity, we impose the constraint that single-particle transitions are inhibited: this corresponds to the assumption that the bound energy of each pair is greater than the energy difference between two adjacent energy levels in the spectrum of the center of mass momentum.
Consider now equation (3.8): we observe that a transition to the first excited state can

be described by an increment of the integer quantum number n_j. As a consequence of the first condition required so far, the transition can be represented by the shift: $n_j \to n_j+1$. It's now immediate to notice, using equation (3.11), that the same process in the center of mass coordinate presents an enhanced increment of the quantum numbers:

$$q_j \to q_j + \frac{2\pi}{L} \implies \sum_{j=1}^{N} q_j \to \sum_{j=1}^{N} q_j + \frac{2\pi}{L} N \tag{3.16}$$

The transitions that we have described so far refer to single particles and still are not related to two-body bound states. Therefore, the grouping of rapidities into pairwise conjugated complex numbers allows us to label the latters with a set of quantum numbers $\tilde{n}_k,\ k = 1, ...N/2$ that keep into account that the n_js of the fermions are pairwise identical in this framework. Explicitly, we can define:

$$\begin{cases} n_{j+1} = n_j \equiv \tilde{n}_k & \text{j odd} \\ n_{j+1} = n_j + 1 & \text{j even} \end{cases} \implies \tilde{n}_{k+1} - \tilde{n}_k = 1 = n_{j+2} - n_j \tag{3.17}$$

Once we have introduced such quantum numbers labelling the strings, we may represent the transition described above for a system of paired fermions as a shift $\tilde{n}_k \to \tilde{n}_k + 1 = \tilde{n}_{k+1},\ \ \forall k = 1, ...N/2$. In both cases j odd and even, we have the following relation with the summation of the quantum number n_j that specify the state of the center of mass momentum:

$$\sum_{j=1}^{N/2} n_{2j} = \sum_{j=1}^{N/2} n_{2j-1} = \frac{1}{2}\sum_{j=1}^{N} n_j = \frac{N}{2} \tag{3.18}$$

We can now explicitly compute the energy of the ground state using (3.13). Introducing $\Lambda = \sum_{j=1}^{N/2} n_{2j-1}$ we have that the corresponding value in the ground state of the system will be:

$$\Lambda^* = \sum_{j=\bar{n}}^{\bar{n}+N/2-1} j = \frac{N(N-2)}{8} + \frac{N}{2}\bar{n}, \tag{3.19}$$

where the second term in the right-hand side depends on N through $\bar{n}$ and fixes the value of Λ^* to the minimum possible value. For instance, we have that for an odd number $N/2$ of pairs $\bar{n} = -(N-2)/4$ and $\Lambda^* = 0$. Therefore, equation (3.19) allows to label the spectrum of the center of mass momentum using a quantum number Λ such that:

$$\Lambda = \Lambda^* + \frac{N}{2} l \quad l \in \mathbb{Z} \tag{3.20}$$

Finally, the energy levels of the system are given by:

$$E_F - E_\Omega^F = \frac{\hbar^2}{2N m_F R^2}\left(\Lambda^* + \frac{N}{2} l - N\frac{\Omega}{\Omega_0}\right)^2 - \frac{m}{\hbar^2}c^2 \frac{N(N-1)(N+1)}{48}, \tag{3.21}$$

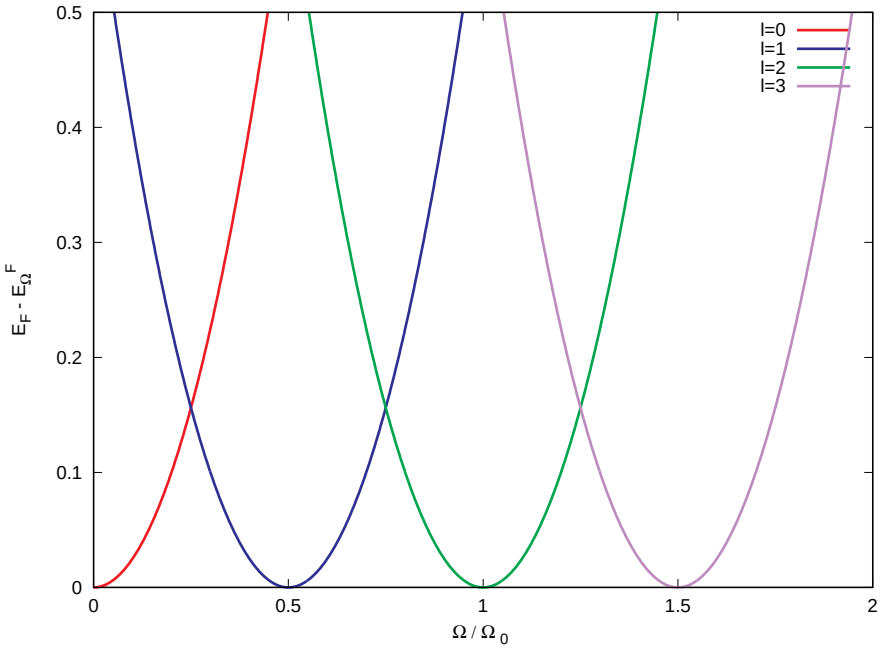

Figure 3.3: Ground state energy (3.21) and first three excited levels in the spectrum as a function of the rescaled rotation frequency Ω/Ω_0 for $N/2 = 9$. Notice the halved periodicity which is due to the formation of pairs.

where we have set $\Omega_0 = \hbar/(m_F R^2)$ and the last term corresponds to the interaction energy.

The persistent current can be now computed using the formula:

$$\mathsf{I}_p = -\frac{\Omega_0}{\hbar}\frac{\partial(E_F - E_\Omega^F)}{\partial\Omega} = \left(\Lambda^* + \frac{N}{2}l - N\frac{\Omega}{\Omega_0}\right) \tag{3.22}$$

From (3.21) one can observe that an increment of 1/2 in the unit element of rotation frequency Ω_0 is equivalent to a transition in the spectrum of the center of mass momentum, displaying a 1/2-periodicity in the latter, as also revealed in Fig.3.3. The very same behaviour is inherited by the persistent current, as can be easily deduced by (3.22). In addition, since the Hamiltonian is totally decoupled in an interaction and in an effective term that depends on Ω, we can infirm that the quantum of artificial gauge flux is the same at any interaction strength. As a second main result, we find that the periodicity of the persistent current of pairs is half of the one of non-interacting fermions for any interaction strength. This is the analog of the case of superconducting pairing, where the periodicity is $\frac{h}{2e}$ as predicted by Byers and Yang in reference [14].

It's worthy to note that the periodicity of the persistent current is univocally defined by the quantum of artificial flux of the components of the gas. Despite in the high interacting bosonic limit of the model, *i.e.* the Tonks-Girardeau gas, such periodicity

coincides with the one of the non-interacting fermions (see Appendix 1), the scaling transformation on the mass leading to the crossover compensates the halving that occurs in the attracting model. Remarkably, this last feature makes the quantum of flux preserves its value during the whole evolution and consequently the periodicity of the persistent current doesn't keep track of the different regimes of the crossover.

Chapter 4

Parity effect

In this section we focus on a mesoscopic effect that occurs in Fermi gases, that is the parity effect. This phenomenon arises when some observable of the system displays a dependence on the number of particles to be even or odd. As it is shown in Appendix A, Bose gases do not undergo the parity effect. Thus, in the system we are studying, we expect that in the strongly attractive bosonic limit such dependence on the number of particles is not observed. In order to properly identify such effect, we start displaying the simpler case of non-interacting spinless fermions confined on a ring and coupled to an artificial gauge field. Then we generalize the analysis to the case involving the attractive contact interactions among fermions. The main difference between the two cases relies on the dependence on N: in the first case the parity effect is conditioned by the number of particles, while in the second one the relevant parameter is the number of pairs $N/2$.

Afterwards, we follow the evolution of the observables affected by the parity effect during the whole BCS-BEC crossover, to detect numerically the continuous weakening of this phenomenon while the system is driven towards the BEC regime. Such further analysis is based on the comparison between the two cases of odd pairs $N = 2$ particles (one pair) and even pairs $N = 4$ particles (two pairs). Once again we obtain results that match the behaviour of Cooper pairs on superconducting rings for which the very same kind of parity effect was obtained via DMRG analysis in ref [35].

4.1 Parity effect: free fermions

We start from a brief and very general review of the theory of a rotating gas of N spinless free fermions of mass m on a ring. The Hamiltonian of the system is:

$$H_{FF} = \sum_{i=1}^{N} \frac{1}{2m}\Big(-i\hbar\frac{\partial}{\partial x_i} - m\Omega R\Big)^2 + E_\Omega^F, \tag{4.1}$$

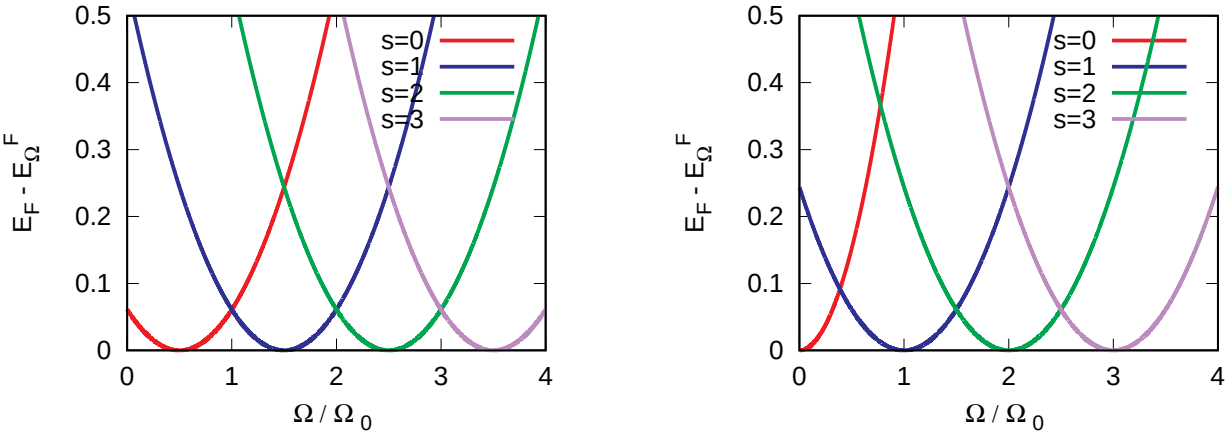

Figure 4.1: Plot of energies of the ground state for N odd (top) and N even (bottom): the relative shift of an half a period is explicitly displayed.

where as in the previous sections, Ω is the angular velocity of the system. The wave-function of the N-body system can be written as a Slater determinant:

$$\Psi_S(x_1..x_N) = \sum_{\mathsf{P}} sgn(\mathsf{P}) \prod_{i=1}^{N} e^{ip_{\mathsf{P}(j)}x_j}, \tag{4.2}$$

where $sgn(\mathsf{P})$ is the sign of the permutation P, belonging to the group of all the possible permutation among the particles. In this case is convenient to include the coupling with the angular veocity in the boundary conditions, applying a twisting phase such that:

$$\Psi_S(0, ...x_N) = e^{i\Omega/\Omega_0}\Psi_S(L, ...x_N) \tag{4.3}$$

where Ω_0 has the same definition provided in Section 3.2. Such boundary conditions yield the following for the rapidities:

$$p_j = \frac{s_j}{R} + \frac{\Omega}{\Omega_0 R}. \tag{4.4}$$

In this case $p_j \in \mathbb{R}$, $\forall j$ and s_j is an integer. The Schroedinger equation yields the following for the energy:

$$E_{FF} - E_\Omega^F = \frac{\hbar^2}{2mR^2} \sum_{j=1}^{N} \Big(s_j + \frac{\Omega}{\Omega_0}\Big)^2 \tag{4.5}$$

In order to obtain the energy of the ground state we have to minimize the following summation:

$$\sum_{j=1}^{N} s_j = \sum_{j=\bar{s}}^{\bar{s}+N-1} j = \frac{N(N-1)}{2} + N\bar{s}$$

This corresponds to choose a proper value for the arbitrary integer $\bar{s} \in \mathbb{Z}$. It's immediate to check that the latter depends on the parity of N. Indeed, for N odd such summation can be set to zero imposing $\bar{s} = -\frac{N-1}{2}$, while for N even the minimum value is reached for $\bar{s} = -\frac{N-2}{2}$ and the summation is non vanishing. We can see that the periodicity of the energy respect to the normalized angular velocity $\frac{\Omega}{\Omega_0}$ is still the same, but there is a shift in the former of a quantity that is exactly half of a period. In order to further analyze the periodicity let's consider the persistent current: using the values of $\bar{s}$ for the two cases and the definition reported in Eq. (3.22) yields

$$I_\Omega = \begin{cases} N\left(s - \frac{\Omega}{\Omega_0}\right), & N \text{ odd} \\ \\ N\left(\frac{1}{2} + s - \frac{\Omega}{\Omega_0}\right), & N \text{ even}, \end{cases} \tag{4.6}$$

where s is an integer that has been introduced to label the quantization of the center of mass momentum, in analogy to what we did in the previous section. From this last relations, we can see that the zeros of the persistent current, which indicate the extremal points of the ground state energy in the cases N even and odd, are shifted by a half of the period as shown in Fig. 4.1. As a consequence, we see that in the lowest energy level the minima and the maxima of the energy evaluated respect to Ω are exchanged. In particular, if the system is in the ground state, we have that, for an odd number of particles, the energy of the non-rotating system $\Omega/\Omega_0 = 0$ is the lowest possible, while for an even number of particles the same condition is associated to the maximum energetic value. In the first case we say that the system displays a diamagnetic behaviour, while in the second case the system is paramagnetic.

In the following, we will show that the parity effect is also present in the model that includes attractive contact interactions between the fermions and furthermore it depends not on the number of particles N but on the number of pairs $N/2$. On the contrary, as it's shown in Appendix A, in the bosonic limit there's no parity effect: the goal of the following section will be to use such property to probe the different regimes of the crossover.

4.2 Parity effect: attractive fermions and crossover

To generalize the results of the previous section to the case of fermions with attractive contact interaction let's consider the persistent current in the ground state Eq.(3.22)

together with (3.19) here reported for sake of convenience:

$$\mathsf{I}_p = \left(\Lambda^* + \frac{N}{2}l - N\frac{\Omega}{\Omega_0}\right)$$

$$\Lambda^* = \sum_{j=\bar{n}}^{\bar{n}+N/2-1} j = \frac{N(N-2)}{8} + \frac{N}{2}\bar{n}$$

As we have already stressed in Chapter 3, Λ^* can be set to zero by imposing $\bar{n} = -(N-2)/4$ if $N/2$ is odd. On the other hand, considering $N/2$ even this is not possible since fermionic quantum numbers can only assume integer values: the second of the previous equation assume the minimum value $\Lambda^* = N/4$ setting $\bar{n} = -(N-4)/4$. These latter considerations shows that there is a parity effect that shifts the zeros of the persistent current of a quantity that is halved respect to the non interacting spinless case described in the previous section. In addition, such effect depends on the number of pairs in the system rather than on the number of particles.

From what we stated so far, we see that the parity effect is strictly related to the possibility of choosing a set of quantum numbers such that the kinetic energy of the center of mass can be set to zero. This is always possible in a bosonic system (see Appendix A for further details) hence there is no parity effect, while in fermionic systems this is possible only for an odd number of components.

In the following we will numerically show that, in the case of $N = 4$, for weakly interacting particles, it is not possible to obtain a ground state wavefunction in Bethe Ansatz form that satisfies periodic boundary conditions imposing a vanishing center of mass momentum. More in detail, the procedure of such numerical analysis has been the following:

- Imposing the center of mass momentum to be zero and periodic boundary conditions on the eigenfunction of the system;
- Using FindRoot algorithm from Mathematica to solve the constraints of the previous point and computing the rapidities that satisfied both conditions;
- Repeated such procedure for several values of the coupling constant, starting from the non-interacting case, then for low interactions and progressively reaching the high interacting regime.

As we have already seen in Section 3.2, the general theory ensures that in the string hypothesis stated so far for infinite systems the rapidities associated to the particles are

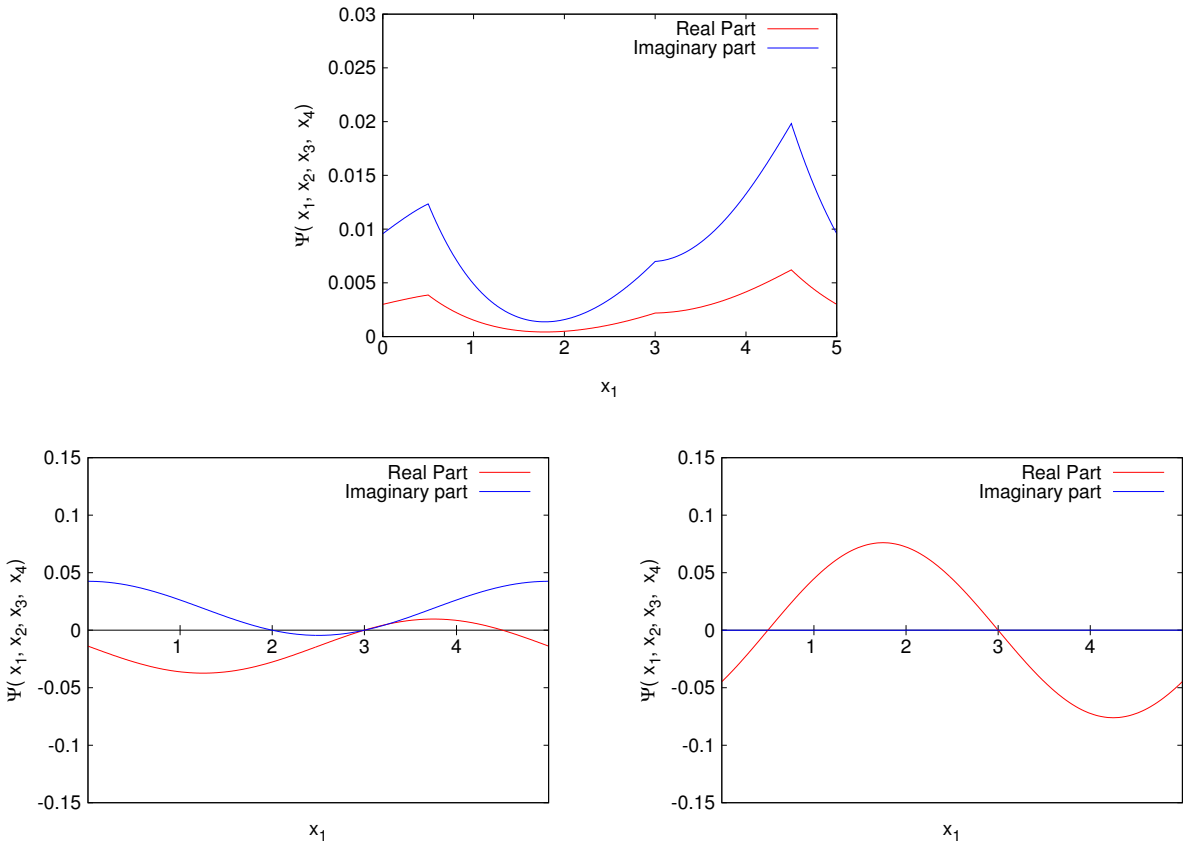

Figure 4.2: Ground state wavefunction for $N = 4$ with strongly attractive interactions c_B (above): the real part of the rapidity is 1.02 π/L and the imaginary one is equal to 0.994 c_B. Notice that both real and imaginary parts are periodic. Wavefunction for the non-interacting system with moving center of mass (left) and static center of mass (right). The one on the left represents the ground state, while the one on the right is an excited state

in the form:

$$k_1^{\pm} = u \pm \frac{C}{2}$$
$$k_2^{\pm} = -u \pm \frac{C}{2},$$

where L is the length of the system and $C = 2m_F/\hbar c$. Since both the number of particles and the number of pairs are even in this case, from what we obtain in Appendix A, if $u = \frac{\pi}{L}l,\ l \in \mathbb{Z}$ we find a bosonic behaviour and thus no parity effect will be detected. On the other hand, if $u = \frac{2\pi}{L}l,\ l \in \mathbb{Z}$ the system is in a fermionic regime and the center of mass momentum cannot be set to zero.

Let's examine the plots in Fig.4.2. In the one above we are in the strong attractive

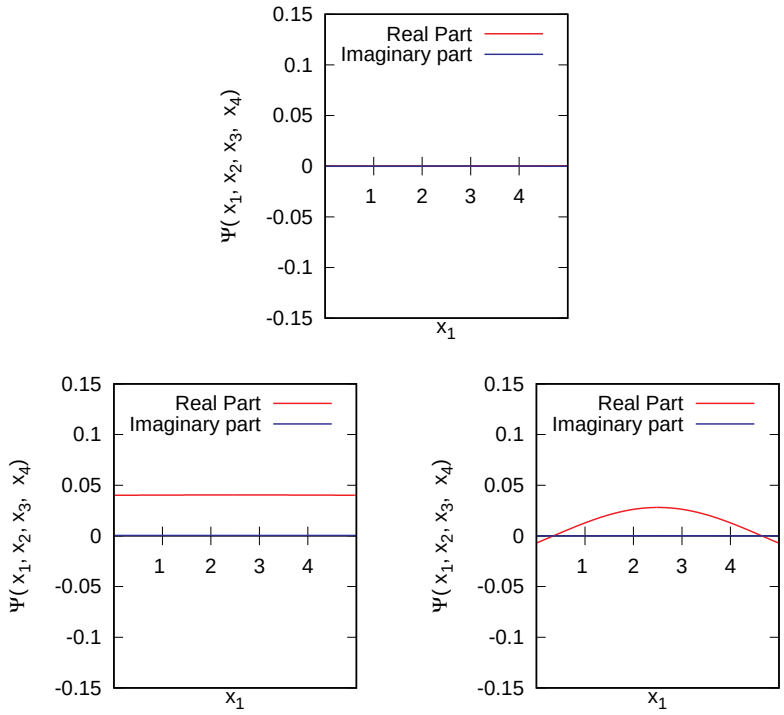

Figure 4.3: Wavefunction in the ground state for zero interactions (above), and weak interactions 10^{-3} (left) and 10^{-2} (right) in unit of the high attractive interactions c_B used in Fig.4.2. The frame of reference with vanishing center of mass momentum is straightforwardly imposed. Starting from the non-interacting model associated with a null eigenfunction, there is a continuous evolution towards the high-interacting regime described in the first plot of Fig.4.2

regime: the rapidities are complex and $u = \frac{\pi}{L}l$. In this regime the momentum of the center of mass of the ground state can be set to zero and there are no parity effects, moreover the imaginary part of the rapidities deviates from the infinite size system.

In the two bottom plots of Fig.4.2 we show the non-interacting wavefunction in two different energy levels. Imposing the center of mass momentum to be zero, one finds that the periodic boundary conditions only provide a non-vanishing wavefunction for real rapidities such that $u = \frac{2\pi}{L}$. Removing the staticity condition for the center of mass one obtains a periodic wavefunction for real rapidities such that $k_1^{\pm} = 0$ and $k_2^{\pm} = 2\pi/L$. Comparing the energy of the two states using $E = \frac{\hbar}{2m}\sum_j (k_j^+)^2 + (k_j^-)^2$ it's immediate to see how the ground state corresponds to the second case. In the non-interacting theory, we find that a vanishing center of mass momentum is coherent with the periodic boundary conditions only in an excited state, while for the ground state this configuration is not possible. As a consequence, we observe the parity effect for non-interacting fermions disappearing once attractive interactions are increased.

In Fig.4.3 we plot the wavefunction of the ground state at weak interactions. What

we see is that imposing the center of mass of the system to be at rest we have a zero wavefunction for the non-interacting theory, then increasing the absolute value of the coupling constant we obtain non-zero wavefunction. Such state continuously evolves towards the high-interacting limit shown in the first plot in Fig.4.2

In conclusion, the numerical results show on one hand that in the non-interacting regime the periodic boundary conditions provide non-zero ground state wavefunction only for a non-vanishing center of mass momentum. This means that in the ground state there will be parity effect, as predicted by the general theory. The same behaviour is inherited when attractive interactions are weakly increased. On the other hand, for higher absolute values of the coupling constant, in the frame of reference in which the center of mass is at rest one has a well-defined wavefunction also in the ground state. This last feature shows how the parity effect disappears at strong interactions.

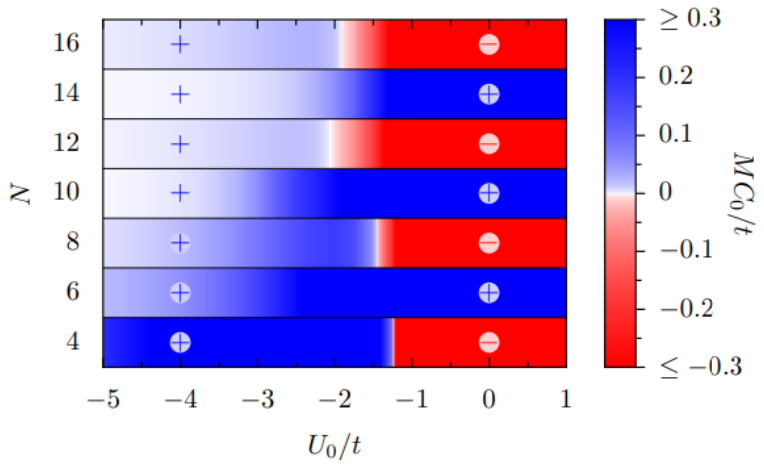

Figure 4.4: DMRG results showing the sign of the second derivative of the energy of the ground state for an attractive Hubbard model as a function of coupling constant U_0/t. We can see that depending on $N/2$ to be odd or even at low interactions we have an interchange between respectively a diamagnetic (blue) and a paramagnetic (red) behaviour, while in the high interacting regime only the diamagnetic behaviour is detected. This is coherent with our analysis of the parity effect in attractive ultracold Fermi gases. Figure from [35].

An interesting remark comes from the comparison between our results and the known theory describing the parity effect on a system of electrons subjected to attractive interactions on a superconducting ring threaded with an external magnetic flux. Indeed, starting from the results obtained in ref.[35] and shown in Fig.4.4, we can see that the DMRG algorithm shows the same interchange between diamagnetic and paramagnetic behaviour depending on the number of pairs in the system. A remarkable difference between our model and the one studied in [35] is the presence of the lattice. A future outlook could be the study of the atomic model in a periodic potential: we would expect that the latter doesn't influence the parity effects.

Conclusions and future outlooks

Summarizing, in this thesis we have studied the exact solution of a model describing a quantum gas of ultracold fermionic atoms subjected to attractive interactions and confined on a strictly one-dimensional ring-shaped potential. In order to study some mesoscopic properties of the system, we have included the coupling with an external artificial magnetic field. Exploiting the integrability of the model, we have provided an exact expression of the many-body wavefunction and of the ground state energy using the Bethe Ansatz. The first result we obtained is the analytical derivation of the periodic behaviour of this latter quantity with respect to the artificial gauge flux. Remarkably, such periodicity is halved if compared to the non-interacting model. This last property is strictly related to the formation of dimers in the ground state of the system. It's also important to underline that the dependence of the ground state energy on the artificial gauge flux reveals the presence of a non-vanishing persistent current in the ring, defined as the derivative of the ground state energy with respect to the flux itself. This latter quantity presents the very same periodic behaviour described so far.

Since the model has been solved at any value of the coupling constant, the analysis of the persistent current can be extended to different interaction regimes and used to probe some typical phenomena occurring in ultracold Fermi gases. In the thesis we focused on the crossover between a system of N weak attractive fermions with mass m_F and the high interacting regime in which the system can be considered as composed by $N/2$ bosons of mass $2m_F$ which strongly repel each other. Such continuous evolution, called BCS-BEC crossover, is univocally driven by increasing the absolute value of the coupling constant and it's formally implemented by a mapping between the ground state energies of the attractive Fermi gas and of the hardcore bosons as shown in ref. [33]. An analysis of the persistent current in the two regimes shows that the period of the latter retains the same value, demonstrating that it doesn't depend on interactions. As a consequence, the periodicity of the current and thus of the ground state energy with respect to the artificial gauge flux doesn't keep track of the different regimes of the system.

In the following chapters we focused on another mesoscopic effect related to the persistent current: the parity effect. Such a phenomenon, that occurs only in fermionic systems, provides a dependence of some observables on the number of components of the gas. In our case, the physical quantity that has been considered is the energy of the

ground state: the parity effect can be detected studying the different response of the gas to the application of the artificial gauge field. There are two possible behaviours whose names come from the analogy with the magnetic systems: diamagnetic and paramagnetic. The first one is determined by an increasing, on a single period, of the energy of the ground state once the artificial gauge field is applied. On the contrary, a paramagnetic behaviour means that after the coupling with the field the system is driven to a more stable configuration and thus on a single period the energy of the ground state decreases.

In this last part, the first result that we obtained is that in the case of attractive fermions the parity effect is related to the number of pairs rather than on the number of particles. If this number is odd the system assumes a diamagnetic behaviour, while if it's even the gas is paramagnetic.

Consequently, we studied the $N = 2$ and $N = 4$ problems and used them to characterize such effect in the presence of attractive interactions. We found that for an odd number of pairs in the non-interacting and low interacting regimes the system behaves like a paramagnet, while at strong attractive coupling between the atoms we observe a diamagnetic response. This is coherent with the behaviour of bosonic systems, as it's shown in Appendix A. We deduce that the parity effect represents a good probe for the different regimes of the BCS-BEC crossover.

Some interesting future outlooks could be the study of the out of equilibrium dynamics of this system to better understand the BCS-BEC crossover in terms of persistent currents. In addition, this kind of analysis could be generalized to more than two species of fermionic atoms, thus including more values for the spin degree of freedom. In this more complicated case, finding an exact solution would require more general techniques than Bethe Ansatz. In order to progressively pursue this target, some useful intermediate steps could include external trapping such as a harmonic or a periodic potential. In such simpler cases, one can exploit some known generalizations [37][38] of Bethe Ansatz for trapped systems in fixed interacting regime to provide further methods for the solution at any coupling strength and thus to fully describe the model.

Appendix A

Tonks Girardeau gas: a Bethe Ansatz solution

Let's now consider a rotating system of N bosons of mass M subjected to strong repulsive contact interaction: we can adapt Hamiltonian (3.6) by setting $g > 0$ and $E_\Omega^B = -1/2 m_B \Omega^2 R^2$. Repeating the procedure followed in the main text, the eigenfunction of the Hamiltonian is:

$$\Phi(\mathbf{x}) = \sum_{\mathsf{P}} A(\mathsf{P}) \exp\Big\{ i \sum_{j=1}^{N} k_{\mathsf{P}(j)} x_j \Big\} \tag{A.1}$$

where in this case the coefficients $A(\mathsf{P})$ are given by:

$$A(\mathsf{P}) = \prod_{\mathbf{T_{kj}}} -e^{i\theta(k_k - k_j)}, \quad A(\mathbb{1}) = 1 \tag{A.2}$$

$$e^{i\theta(k_k - k_j)} = \frac{\frac{2m_B g}{\hbar^2} - ik_k + ik_j}{\frac{2m_B g}{\hbar^2} + ik_k - ik_j} \tag{A.3}$$

Since we are considering a strong repulsive interaction, we can consider the limit $g \to \infty$ of the last relations:

$$\lim_{g\to\infty} e^{i\theta(k_k - k_j)} = \frac{\frac{2m_B g}{\hbar^2} - ik_k + ik_j}{\frac{2m_B g}{\hbar^2} + ik_k - ik_j} = 1 \to \theta(k_k - k_j) = 0 \tag{A.4}$$

$$A(\mathsf{P}) = \prod_{T_{ij}} (-1) \quad \forall \mathsf{P} \tag{A.5}$$

Requiring the periodicity of the boundary conditions one obtains the following equation to be satisfied by the rapidities:

$$\exp\{ik_jL\} = (-1)^{N-1} \implies k_j = \frac{2\pi}{L}\Big(\frac{N-1}{2} + r_j\Big) \quad r_j \in \mathbb{Z} \tag{A.6}$$

It's important to stress that since we are considering repulsive interactions, the rapidities k_j are real numbers $\forall j = 1...N$. As a consequence, in this case we don't need to split the energy eigenvalues in an bound and effective contributions thus it's not necessary to introduce the center of mass and relative coordinates. A direct computation of the energy of the system yields:

$$E_B = \frac{\hbar^2}{2m_B}\sum_{j=1}^{N} k_j^2 + E_\Omega^B = \frac{\hbar^2}{2m_BR^2}\sum_{j=1}^{N}\Big(r_j + \frac{N-1}{2} + \frac{\Omega}{\Omega_0'}\Big)^2 + E_\Omega^B, \tag{A.7}$$

where $\Omega_0' = \frac{\hbar}{m_BR^2}$. It's important to observe that we can define a new set of quantum numbers, depending on N, that label the energy levels. Indeed let's introduce $\Gamma_j = r_j + \frac{N-1}{2}$: it's immediate to check that for odd N we have $\Gamma_j \in \mathbb{Z}$, while Γ_j is a semi-integer for even N . From equation (A.7) we see that an increment $\Omega \to \Omega + \Omega_0'$ induces a shift in each quantum number Γ_j, showing a periodic behaviour of the energy with respect to the rotation frequency. In order to obtain the ground state of the system we have to choose the quantum numbers that make (A.7) assume its minimum value. Similarly to what we have done in the main text, we fix the conditions:

$$\begin{cases} \Gamma_{j+1} - \Gamma_j = 1 \\ \Gamma_1 = \tilde{\Gamma} \end{cases} \tag{A.8}$$

Where $\tilde{\Gamma}$ is the integer or the semi integer depending on N that, taking into account the first of the conditions (A.8) minimizes (A.7). As a consequence, the latter can be recast in the following form:

$$E_B - E_\Omega^B = \frac{\hbar^2}{2m_BR^2}\sum_{j=0}^{N-1}\Big(\tilde{\Gamma} + j + \frac{\Omega}{\Omega_0'}\Big)^2 \tag{A.9}$$

It is now possible to calculate the value of the persistent current by keeping the value of E_Ω^B fixed:

$$\mathsf{I}_p' = -\frac{\Omega_0'}{\hbar}\frac{\partial(E_B - E_\Omega^B)}{\partial\Omega} = \sum_{j=1}^{N-1}\Big(\tilde{\Gamma} + j\Big) + N\frac{\Omega}{\Omega_0'} \tag{A.10}$$

From this last expression we see that also the persistent current shows the same periodic behaviour of the energy respect to the angular velocity. It's important to stress

that such periodicity doesn't depend on the number of particles N and coincides with the one of the non interacting fermions.

A further point that has to be discussed concerns the quantum numbers of the system. We have seen that

for odd number of particles Γ_js are integer, while for even N they assume half-integer values. As a consequence, if we consider the center of mass momentum of the particles defined by:

$$K_{COM} = \frac{2\pi}{L} \sum_{j=1}^{N} \Gamma_j, \tag{A.11}$$

we see that, as opposed to what we found in Section 4.2, such summation can be set to zero choosing a proper value for $\tilde{\Gamma}$ both for even and odd number of particles. This implies that in the case of a Bose gas we don't expect any shift neither in the energy of the ground state nor in the persistent current depending on N and thus no parity effect should be detected.

Appendix B

Two particle problem

Consider two fermions, one spin up and one spin down, interacting via a delta-potential on a 1-dimensional interval of lenght L. The Hamiltonian of the system is:

$$H = -\frac{\hbar^2}{2m}\Big(\frac{\partial^2}{\partial x_1^2} + \frac{\partial^2}{\partial x_2^2}\Big) + g\delta(x_2 - x_1) \tag{B.1}$$

To solve the associated Schroedinger equation, consider the Ansatz:

$$\begin{aligned}\Psi(x_1, x_2) = \theta(x_1 - x_2)\Big(A_{11}e^{ik_1x_1+ik_2x_2} + A_{12}e^{ik_2x_1+ik_1x_2}\Big)+ \\ + \theta(x_2 - x_1)\Big(A_{21}e^{ik_2x_1+ik_1x_2} + A_{22}e^{ik_2x_2+ik_1x_1}\Big),\end{aligned} \tag{B.2}$$

where A_{ij} are complex coefficients and k_i are the rapidities of the two particles. Notice that since the two fermions have different spin there is no constraint of antisymmetry of the wavefunction. Indeed, it has been shown[36] that the ground state of this model is actually the most symmetric one. In the following we will impose an appropriate number of conditions on the spatial structure of the eigenfunction in order to determine all the coefficients A_{ij} and to find an expression for the rapidities.

- Symmetry under exchange of the two particles;
- Discontinuity of the first derivative of the wavefunction;
- Normalization constraint;
- Periodic boundary conditions;

Symmetry respect to the exchange of the two particles

Using the expression (B.2) it's immediate to obtain:

$$\begin{aligned}
&\Psi(x_1,x_2)=\Psi(x_2,x_1) \implies \\
&\theta(x_1-x_2)\Big(A_{11}e^{ik_1x_1+ik_2x_2}+A_{12}e^{ik_2x_1+ik_1x_2}\Big)+\theta(x_2-x_1)\Big(A_{21}e^{ik_2x_1+ik_1x_2}+A_{22}e^{ik_2x_2+ik_1x_1}\Big)= \\
&\theta(x_2-x_1)\Big(A_{11}e^{ik_1x_2+ik_2x_1}+A_{12}e^{ik_2x_2+ik_1x_1}\Big)+\theta(x_1-x_2)\Big(A_{21}e^{ik_2x_2+ik_1x_1}+A_{22}e^{ik_2x_1+ik_1x_2}\Big) \implies \\
&A_{11}=A_{21}\cup A_{22}=A_{12}
\end{aligned} \tag{B.3}$$

Discontinuity of the first derivative of the eigenfunction

Let's introduce the center of mass and relative coordinate of the particles:

$$\begin{cases} R=(x_1+x_2)/2 \\ r=x_2-x_1 \end{cases} \tag{B.4}$$

In this frame of coordinates, the spatial component of eigenfunction (B.2) can be recast as:

$$\Psi(R,r)=\theta(-r)e^{iK_cR}\Big(A_{11}e^{ik_rr}+A_{12}e^{-ik_rr}\Big)+\theta(r)e^{iK_cR}\Big(A_{21}e^{-ik_rr}+A_{22}e^{ik_rr}\Big) \tag{B.5}$$

where the transformed rapidities $k_r=\frac{k_2-k_1}{2},\ K_c=k_1+k_2$ have been defined.

The discontinuity of the first derivative caused by the contact interaction can be written explicitly as:

$$\begin{aligned}
&\frac{\partial\Psi}{\partial r}(R,r=0^+)-\frac{\partial\Psi}{\partial r}(R,r=-0^-)=c_2\Psi(R,r=0)\rightarrow \\
&\rightarrow(A_{22}+A_{12}+A_{12}-A_{11})ik_r=c_2(A_{22}+A_{12}+A_{12}+A_{11}),\quad c_2=\frac{2m}{\hbar}g
\end{aligned} \tag{B.6}$$

Substituting the symmetry condition (B.3) one obtains the following relation:

$$A_{22}=-A_{11}\frac{c_2-i(k_1-k_2)}{c_2+i(k_1-k_2)} \tag{B.7}$$

Eventually, the coefficient A_{11} can be fixed by requiring the eigenfunction to be normalized, thus apart from a moltiplicative constant can be set equal to one.

Periodic Boundary Conditions

Summarizing, as a consequence of the constraints imposed so far, the eigenfunction can be written as:

$$\Psi(x_1,x_2) \propto \theta(x_1-x_2)\Big(e^{ik_1x_1+ik_2x_2} - \frac{c_2-i(k_1-k_2)}{c_2+i(k_1-k_2)}e^{ik_2x_1+ik_1x_2}\Big)+$$
$$+\,\theta(x_2-x_1)\Big(e^{ik_2x_1+ik_1x_2} - \frac{c_2-i(k_1-k_2)}{c_2+i(k_1-k_2)}e^{ik_2x_2+ik_1x_1}\Big) \tag{B.8}$$

Periodic boundary conditions read:

$$\Psi(x_1=0,x_2) = \Psi(x_1=L,x_2) \tag{B.9}$$

After a straightforward substitution and using the property of the Theta function we obtain:

$$(1+\frac{c_2-i(k_1-k_2)}{c_2+i(k_1-k_2)})e^{ik_2L})e^{ik_1x_2} + (-\frac{c_2-i(k_1-k_2)}{c_2+i(k_1-k_2)} - e^{ik_1L})e^{ik_2x_2} = 0 \tag{B.10}$$

Assuming $k_1 \neq k_2$ we have that the two terms in the last equation are linear independent: each of them must identically vanish. As a consequence, we obtain the two following conditions for the rapidities:

$$e^{-ik_1L} = -\frac{c_2-i(k_2-k_1)}{c_2+i(k_2-k_1)} \tag{B.11}$$

$$e^{-ik_2L} = -\frac{c_2-i(k_1-k_2)}{c_2+i(k_1-k_2)} \tag{B.12}$$

It's worthy to notice that the rapidity of the center of mass of the system does not depend on interactions:

$$e^{i(k_1+k_2)L} = e^{iK_cL} = 1$$

Consider now the structure of the eigenfunction (B.8). Each sector of coordinates is composed by two plane waves that, apart from a phase shift that keeps into account the contact interaction, differ for a permutation of the rapidities. We can associate to the former $e^{ik_1x_1+ik_2x_2}$ the permutation $P_1 = \mathbb{1}$ acting on $k_{1,2}$ and to the second plane wave the permutation $P_2 : (k_1,k_2) \to (k_2,k_1)$. Now we introduce the factor:

$$-e^{i\phi(k_i-k_j)} = -\frac{c_2 - i(k_i - k_j)}{c_2 + i(k_i - k_j)}, \tag{B.13}$$

where k_j is the rapidity associated to the maximum between x_1 and x_2 in each sector. It's immediate to check from (B.8) that this phase maps each term of the eigenfunction in the other sector of coordinates, in the term that corresponds to the same permutation of the rapidities. Under this condition, the wavefunction can be recast by considering only one sector of coordinates:

$$\Psi_{BA}(x_1, x_2) = \sum_P A(P) \exp\{i \sum_{j=1}^{N} k_{P(j)} x_j\} \tag{B.14}$$

Where $A(P) = A_{11}$ if $P = \mathbb{1}$ and $A(P) = A_{22}$ if P is the permutation that inverts the rapidities of the particles. The other sector of coordinates can be studied by using the unitary transformation (B.13). As a consequence, the periodic boundary conditions in this new frame can be equivalently expressed in the form:

$$\sum_P A(P) \exp\{i \sum_{j\neq 1}^{N} k_{P(j)} x_j\} = \sum_P A(P) \exp\{i \sum_{j\neq 1}^{N} k_{P(j)} x_j\} \exp\{i k_{P(j)} L\} \Big(-e^{i\phi(k_i-k_j)}\Big),$$

where the phase term in the right-hand side maps the first sector of coordinates in the second one.

From this expression it's immediate to see the equivalence with the Bethe Ansatz, expressed also by equations (B.11) and (B.12) that coincide with the Bethe equations for the same model.

In order to obtain the solution for the finite ring, we have numerically solved the coupled equations (B.11) and (B.12). This has been performed using a root-finding algorithm. The program has been written in Mathematica, using NSolve algorithm to find the imaginary part of the rapidities and assuming that k_1 was the complex conjugate of k_2 in order to have real-valued energy eigenvalues.

Bibliography

[1] M.H. Anderson, J.R. Ensher, M.R. Matthews, C.E. Wieman, E.A. Cornell, Science, Vol. 269, Issue 5221, pp. 198-201 (1995);

[2] L. Amico et al., New J. Phys. 19 020201 (2017);

[3] V. Galitski et al., Phys. Today 72, 1, p. 38 (2019);

[4] S. Butera et al., New J. Phys. 18 085001 (2016);

[5] C. Ryu , M.G. Boshier, New J. Phys. 17 092002 (2015);

[6] S. Pandey, Nature, Vol. 570, pp 205–209 (2019);

[7] W. Zwerger, The BCS-BEC Crossover and the Unitary Fermi Gas. Lecture Notes in Physics, Springer (2011);

[8] D.S. Petrov, C. Salomon, G.V. Shlyapnikov, Phys. Rev. Lett. 93 (2004);

[9] C. Chin, R. Grimm, P. Julienne, E. Tiesinga, Rev. Mod. Phys. 82, 1225 (2010);

[10] J.N. Fuchs, A. Recati, W. Zwerger, Phys. Rev. Lett. 93, 090408 (2004);

[11] H. Bethe, Z. Physik 71, 205 (1931);

[12] M. Gaudin, Phys. Lett. 24A, 55 (1967);

[13] C.N. Yang, Phys. Rev. Lett. 19, 1312 (1967);

[14] N. Byers, C. N. Yang, Phys. Rev. Lett. 7, 46 (1961);

[15] B.P. Anderson, M.A. Kasevich, Science, Vol. 282, 5394, pp. 1686-1689 (1998);

[16] M. Azuma et al., Phys. Rev. Lett. 73, (1994);

[17] G. Gauthier, I. Lenton, N. McKay Parry, M. Baker, M. J. Davis, H. Rubinsztein-Dunlop, T.W. Neely, Optica, Vol. 3, Issue 10, pp. 1136-1143 (2016);

[18] M. A. Cazalilla, R. Citro, T. Giamarchi, E. Orignac, M. Rigol, Rev. Mod. Phys. 83, 1405 (2011);

[19] Maxim Olshanii, Phys. Rev. Lett., Vol. 81, p. 938 (1998);

[20] Barry R. Holstein, American Journal of Physics 69, 441 (2001);

[21] S.C. Caliga et al., New J. Phys. 18 015012 (2016);

[22] A. Ramanathan et al. Phys. Rev. Lett. 106, 130401 (2011);

[23] A.C. Mathey and L. Mathey, New J. Phys. 18 055016 (2016);

[24] B. DeMarco, D.S. Jin, Science, Vol. 285, Issue 5434, pp. 1703-1706 (1999);

[25] C. Chin et al., Science, Vol. 305, Issue 5687, pp. 1128-1130 (2004);

[26] I. Ferrier-Barbut et al., Science, Vol. 345, Issue 6200, pp. 1035-1038 (2014);

[27] A. Bohr, B.R Mottelson, D. Pines, Phys. Rev. 110, 936 (1958);

[28] D. Vollhardt, P. Wölfle, Taylor and Francis, London (1990);

[29] P. Nozières, S.J. Schmitt-Rink, Low. Temp. Phys. 59, 195 (1985);

[30] M. Büttiker, Y. Imry, R. Landauer, Phys. Lett. 96A, 365 (1983).

[31] A. J. Leggett, Granular Nanoelectronics, edited by D. K. Ferry, pp. 297–311, Plenum Press (1991);

[32] E.H.Lieb, W. Liniger, Phys. Rev. 130 (1963);

[33] M.Wadati, Journal of the Physical Society of Japan, Vol. 71, No. 11, pp. 2657–2662 (2002);

[34] J.B McGuire, J. Math. Phys. 5, 622 (1964);

[35] X. Waintal et al. Phys. Rev. Lett. 101, (2008);

[36] J. Decamp, P. Armagnat, B. Fang, M. Albert, A. Minguzzi, P. Vignolo, New J. Phys., 18, 055011 (2016);

[37] M. D. Girardeau, E. M. Wright, Phys. Rev. Lett. 84, 5239 (2000);

[38] A.G. Volosniev et al., Nat. Phys. 5, 5300 (2014).

Acknowledgements

First of all, I would like to thank Prof. Elisa Ercolessi and Dr. Anna Minguzzi for the great help and inspiration that were fundamental to give birth to this thesis. In particular, I would like to thank Prof. Ercolessi for assisting and encouraging me to enrich my personal and academic experience with a study period abroad. I would like to acknowledge Dr. Anna Minguzzi for introducing me to the complicated and fascinating world of scientific research, on one side transmitting me her expertise in the field and on the other side pushing me to continuously deepen my understanding and comprehension of the topics I was facing, steering me in the right direction whenever needed.

I would like to express my gratitude to Professor Luigi Amico, for the very useful discussions and the important cues that in several occasions provide new and intriguing prospectives to my research. I would like to acknowledge Dr. Piero Naldesi for the fruitful debates about physics and the topics of my thesis. I also would like to thank Piero for the huge support and help in my adaptation in a new city and a new environment.

I'm grateful to all the LPMMC guys and staff for the beautiful and stimulating atmosphere I've been in for the last semester.

I would like to thank my family, starting from my parents, for all the sacrifices and the efforts done to allow me to reach this point. None of this would have been possible without them.

Last but not least, I would like to thank all the people that during all the years as a university student allow me to have the peace of mind necessary to go through this beautiful experience. The entire list would be too long, so I will just thank all the people that have spent time in Via del Porto 1 especially who, year after year, found between those walls a place to call home.